Available online at www.sciencedirect.com
SCIENCE DIRECT
Journal of Asian Earth Sciences 28 (2006) 20–37
Journal of Asian Earth Sciences
www.elsevier.com/locate/jaes

Metamorphic evolution of high-pressure and ultrahigh-temperature granulites from the Highland Complex, Sri Lanka

Yasuhito Osanai [a,*], Krishnan Sajeev [b], Masaaki Owada [c], K.V.Wilbert Kehelpannala [d], W.K.Bernard Prame [e], Nobuhiko Nakano [a], Sarath Jayatileke [f]

[a] *Division of Evolution of Earth Environments, Graduate School of Social, Cultural Studies, Kyushu University, Fukuoka 810-8560, Japan*
[b] *Research Institute of Natural Sciences, Okayama University of Science, Okayama 700-0005, Japan*
[c] *Department of Earth Science, Yamaguchi University, Yamaguchi 753-8512, Japan*
[d] *Institute of Fundamental Studies, Hantana Road, Kandy, Sri Lanka*
[e] *Geological Survey and Mines Bureau, Dehiwala, Sri Lanka*
[f] *Industrial Technology Institute, Colombo 7, Sri Lanka*

Received 16 December 2003; received in revised form 24 May 2004; accepted 24 September 2004

Abstract

Sapphirine + quartz-bearing pelitic granulites, garnet–clinopyroxene–quartz-bearing mafic granulites and quartzo-feldspathic granulites with corundum–garnet–quartz constitute rare but important members of the Highland Complex in Sri Lanka. Peak metamorphic conditions from the Highland Complex generally have been considered to be up to ~850–900 °C and ~8 10 kbar. However, this study on the above mentioned rocks indicates that ultrahigh-temperature and high-pressure conditions (>1100 °C and ~12 kbar) were attained during peak conditions. A metamorphic evolution of the ultrahigh-temperature metamorphic rocks was determined from careful analyses of shifts in divariant assemblages and reaction textures. This shows a clockwise P–T path from more high-pressure conditions (~1000 °C and ~17 kbar; stage 0 as part of the prograde metamorphic path) to lower-pressure and -temperature conditions (~950 °C and ~9 kbar; stage 4 as part of the retrograde path) through the peak metamorphic conditions (stage 1). Widespread lower pressure and temperature granulite-facies metamorphic rocks surround the ultrahigh-temperature granulites and are interpreted to have formed by the strong effect of the retrograde metamorphism and deformation. The widely reported Pan-African metamorphic ages derived from similar granulite-facies metamorphic rocks in the Gondwana fragments (Highland Complex in Sri Lanka, Lützow-Holm Complex in east Antarctica, etc.) may also be the result of retrograde metamorphism of ultrahigh-temperature metamorphic rocks. There remains a possibility that this early ultrahigh-temperature/high-pressure granulite-facies metamorphism in the Highland Complex, as well as that in the Lützow-Holm Complex, might pre-date Pan-African metamorphism.

Keywords: High-pressure mafic granulite; UHT-pelitic granulites; Clockwise P–T path; Highland Complex; Sri Lanka

1. Introduction

The Sri Lankan metamorphic basement has been subdivided into three major units, namely, the Vijayan Complex in the east, the Highland Complex in the central and the Wanni Complex in the west (Kehelpannala, 1997; Fig. 1). The basis for this new subdivision is Nd-model age determinations covering the entire basement (Milisenda et al., 1988; Kröner et al., 1991; Liew et al., 1991). The Vijayan Complex consists mainly of amphibolite-facies granitoid rocks, metadiorites, metagabbros and migmatites (e.g. Cooray, 1984; Kröner et al., 2003; Kehelpannala, 2004), while the Highland Complex is composed of pelitic, mafic and quartzo-feldspathic granulites, abundant charnockitic rocks, marble and quartzite, all metamorphosed to granulite-facies conditions. Some of these granulites contain ultrahigh-temperature assemblages. Rocks in the Wanni Complex are metapelites, metasemipelites, quartzites, charnockites, metagabbro, metadiorite, and meta-granitoids and are metamorphosed to upper amphibolite to granulite facies conditions. Characteristic arrested charnockites can also be found in the Wanni Complex (e.g. Hansen et al., 1987; Hiroi et al., 1990, 1994; Ogo et al., 1992; Kehelpannala, 1999).

* Corresponding author. Fax: +81 92 726 4843.
E-mail address: osanai@scs.kyushu-u.ac.jp (Y. Osanai).

1367-9120/$ - see front matter © 2006 Elsevier Ltd. All rights reserved.
doi:10.1016/j.jseaes.2004.09.013

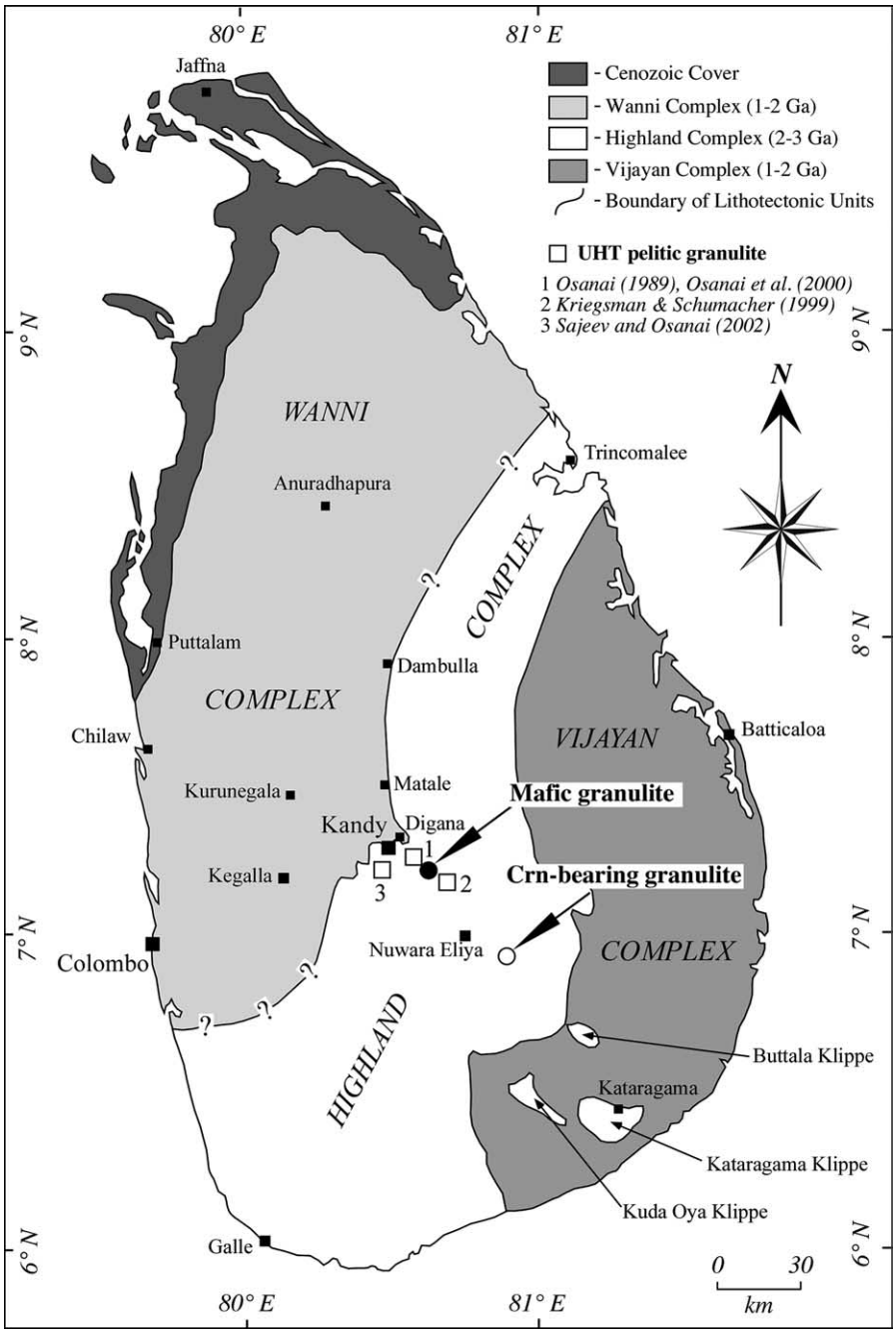

Fig. 1. Lithotectonic map of the Sri Lankan metamorphic basement modified after Kehelpannala (1997). Sample locations of studied ultrahigh-temperature metamorphic rocks are shown as open squares, open circle and black circle.

The boundary between the Highland Complex and the Vijayan Complex is a tectonic contact with strong shearing and thrusting (e.g. Kleinschrodt, 1994). Recent work by Kehelpannala (1997, 2003, 2004) suggests that the boundary between the Highland and Wanni Complexes is a crustal-scale shear zone, part of which is the Digana shear zone. Another small complex called the Kadugannawa Complex (Kröner et al., 1991; Cooray, 1994), which was known as 'Arenas' (Vitanage, 1972; Almond, 1991) (Arenas are doubly plunging synforms), has also been recognized in the northwestern part of the Kandy area between the Wanni Complex and the Highland Complex. Based on geology, geochronology and structure, the Kadugannawa Complex is now regarded as part of the Wanni Complex (Kehelpannala, 1991, 1997; Kröner et al., 2003), and amphibolites, metagabbros and metadiorites occurring within these doubly plunging synforms may represent a Neoproterozoic magmatic arc (Willbold et al., 2004; Kehelpannala, 2004).

The metamorphic basement of Sri Lanka has been considered as a key terrain to understand the evolution of the Gondwana supercontinent since the island was geographically located close to India, Madagascar and East Antarctica as the main portions of East Gondwanaland. Grenvillian and Pan-African events have been distinctly developed in the Highland

Complex (e.g. Kröner et al., 2003; Kehelpannala, 2003; Yoshida et al., 2003) during its evolution since the Palaeoproterozoic similar to the situation in Peninsular India and in other Gondwana fragments.

Peak metamorphic conditions of widespread granulite-facies metamorphic rocks from the Highland Complex have been estimated to be up to ~850–900 °C and ~8–10 kbar (e.g. Schumacher et al., 1990; Raith et al., 1991; Kriegsman, 1991; Schenk et al., 1991; Hiroi et al., 1994; Raase and Schenk, 1994; Schumacher and Faulhaber, 1994; Kriegsman and Schumacher, 1999). As shown in various petrogenetic grids, mineral assemblages in pelitic rocks are highly sensitive to changing physical conditions, especially at high- to ultrahigh-temperature conditions. Therefore, these pressure–temperature conditions might represent overprinting of higher-grade assemblages in rocks with pelitic composition during retrograde metamorphism. However, rarely sapphirine + quartz-bearing granulites are preserved as blocks or lenses in other metamorphic rocks, which indicate ultrahigh-temperature conditions (> 1050 °C, ~12 kbar) prevailed in the Highland Complex (e.g. Osanai et al., 2000; Sajeev and Osanai, 2004a).

Changes in mineral assemblages of mafic metamorphic rocks are not so clear under high- to ultrahigh-temperature conditions, which indicate only differences in the pressure, for example, between high-pressure eclogite-facies (orthopyroxene- and plagioclase-free garnet–clinopyroxene–quartz assemblages) and moderate- to low-pressure granulite-facies (orthopyroxene- and plagioclase-bearing assemblages) conditions. Generally, retrograde effects of granulite-facies mafic rocks are understood by the formation of late hydrous minerals such as hornblende.

Variation of mineral assemblages (including aluminosilicates, corundum, spinel and quartz) and reaction textures in aluminous quartzo-feldspathic granulites are also useful to determine the evolution under ultrahigh-temperature conditions. Therefore, we combine changes in available divariant mineral assemblages and reliable reaction textures in pelitic, mafic and aluminous quartzo-feldspathic metamorphic rocks to determine the highest-grade metamorphic conditions and metamorphic evolution of the Highland Complex of Sri Lanka.

In this paper, we discuss a possible pressure–temperature evolution for mafic (garnet–clinopyroxene–orthopyroxene granulite), magnesium and aluminous pelitic (sapphirine-bearing garnet–orthopyroxene–cordierite–sillimanite gneiss and sapphirine–garnet–orthopyroxene granulite), and aluminous quartzo-feldspathic (corundum–garnet–sillimanite–spinel gneiss) metamorphic rocks exhibiting ultrahigh-temperature/-high-pressure reaction textures from the central Highland Complex. A comparison on the metamorphic evolution of ultrahigh-temperature granulites between the Highland Complex and the other well known high-grade metamorphic terrain of the Lützow–Holm Complex in east Antarctica, both of which were derived from Gondwana supercontinent, will also be discussed shortly.

2. General geology and modes of occurrence of ultrahigh-temperature granulites in the Highland Complex

Rocks exhibiting ultrahigh-temperature assemblages occur mostly as blocks, disrupted layers or lenses at various localities in the central part of the Highland Complex. Recent studies have also identified other spinel + quartz-bearing and osumilite-bearing high-grade assemblages from the southwestern part of the Highland Complex (Osanai et al., 2000; Sajeev and Osanai, 2004b). In this contribution, we will describe the modes of occurrence of some selected ultrahigh-temperature metamorphic rocks from the central part of the Highland Complex. The distribution of the studied localities is shown in Fig. 1.

2.1. Ultrahigh-temperature mafic granulites

The mafic granulite (garnet–clinopyroxene–orthopyroxene granulite) samples studied were collected from a roadside exposure on the road leading to the Victoria Dam towards the southeastern part of Kandy. The mafic granulite is seen as lenses or blocks (about 2–3 m long and 1 m wide) within layered pelitic (khondalitic) granulites (garnet–sillimanite–cordierite–biotite ± graphite gneiss and garnet–biotite gneiss) (Fig. 2a and b) and calc-silicate rocks. In the hand specimen itself, reddish garnet and greenish clinopyroxene and quartz porphyroblasts are visible to the naked eye. Fine symplectites of orthopyroxene–plagioclase can also be identified at the grain boundaries of porphyroblasts. It was noted that the mafic granulites show minor variation of their lithology due to the modes of constituent minerals. The foliation varies from N 50° W to N 5° E with a dip of 75–85° S and seems to be parallel to the adjacent layers of pelitic garnet–sillimanite–cordierite–biotite gneisses.

2.2. Ultrahigh-temperature magnesium and aluminous pelitic gneisses and granulites

The sapphirine-bearing garnet–orthopyroxene–cordierite–sillimanite gneisses are exposed along the roadside and in a quarry near the Kotmale reservoir towards the south of Gampola (Fig. 2c and d). These granulites are observed as intercalations within pelitic gneisses, two-pyroxene mafic granulite and charnockite. The related pelitic rocks consist mainly of garnet–cordierite–sillimanite–spinel–graphite gneiss (khondalite), garnet–biotite gneiss and garnet-bearing orthopyroxene–sillimanite gneiss. The sapphirine-bearing garnet–orthopyroxene–cordierite–sillimanite gneisses are relatively fresh and occur as thin layers including porphyroblasts of garnet surrounded by sillimanite, orthopyroxene and cordierite. Porphyroblasts of orthopyroxene associated with sillimanite can also be identified to the naked eye. The rocks in this exposure are well foliated with a general trend of N 5° W and a dip of 38–50° towards W. Sajeev and Osanai (2004a) described more detail on the mode of occurrence of the gneiss.

The sapphirine–garnet–orthopyroxene granulites are exposed in a marble quarry at Ampitiya, near Kandy (Fig. 2e

Fig. 2. Modes of occurrence of ultrahigh-temperature metamorphic rocks from the Highland Complex. (a) roadside exposure of garnet–clinopyroxene–orthopyroxene–bearing mafic granulite as thin intercalation in layered pelitic gneisses near Victoria Dam, (b) close-up view of mafic granulite. Melanocratic bands are rich in retrograde hornblende, (c) roadside exposure of sapphirine-bearing garnet–orthopyroxene–sillimanite gneiss near Gampola, (d) close-up of sapphirine-bearing garnet–orthopyroxene–sillimanite gneiss, (e) sapphirine–garnet–orthopyroxene granulite exposure as blocks in pure marble near Ampitiya, (f) close-up view of sapphirine–garnet–orthopyroxene granulite, (g) thin band of corundum–garnet–sillimanite–spinel gneiss in layered pelitic gneisses near Welimada, (h) close-up of corundum–garnet–sillimanite–spinel gneiss.

and f) (Osanai, 1989; Osanai et al., 2000). Osanai (1989) discovered the first sapphirine occurrence in Sri Lanka from this locality. Even though various localities of very high-grade, ultrahigh-temperature assemblages have been identified later, this locality is still very important because of the presence of a wide range of mineral assemblages in the rock. These very high-grade granulites in this exposure are identified as blocks within the Highland marble. The size of the blocks varies from centimeter scale to meter scale. The host marble is almost pure with rare occurrences of corundum and spinel. Olivine

and phlogophite are also present in certain domains. A rare occurrence of garnet-free sapphirine–orthopyroxene–cordierite granulite is also identified, which is relatively fine-grained, compared to that of sapphirine–garnet–orthopyroxene granulite. Blocks (up to 1 m in diameter) of mafic granulites are also seen at this locality. These mafic granulite blocks are almost similar to the mafic granulite explained above.

2.3. Ultrahigh-temperature aluminous quartzo-feldspathic gneiss

Highly aluminous corundum–garnet–sillimanite–spinel gneiss is exposed in a quarry on a roadside near Welimada, southeast of Nuwara Eliya (Fig. 2g and h). The exposure consists mainly of charnockite with thin layers of quartzo-feldspathic gneiss, pelitic gneiss and hornblende-bearing mafic granulite. The corundum–garnet–sillimanite–spinel gneiss is observed as thin layers (up to 20 cm in width) in contact with garnet–biotite gneiss, garnet–sillimanite–biotite gneiss and garnet–orthopyroxene gneiss. The foliation trend is N 20° E with a gentle eastward dip ($\sim$30°).

3. Petrographical features and mineral chemistry

In this section, we describe petrographic and mineral chemical characteristics of the following three types of ultrahigh-temperature metamorphic rocks from the central Highland Complex: (1) Mafic metamorphic rocks are garnet–clinopyroxene–orthopyroxene granulites (samples 010501B1–B3). These rocks contain some reaction textures from high-pressure condition down to moderate-pressure. (2) Magnesium and aluminous pelitic metamorphic rocks are sapphirine-bearing garnet–orthopyroxene–cordierite–sillimanite gneisses (123107B, 10101H) containing characteristic sapphirine–quartz coexistence as inclusion in garnet and sapphirine–garnet–orthopyroxene granulites (71501A–E), which show some retrograde reaction textures. (3) Aluminous quartzo-feldspathic metamorphic rocks are corundum–garnet–sillimanite–spinel gneisses (121603I1–I4) containing distinctive corundum–quartz coexistence and some reaction textures inferred to record decompression and cooling.

Mineral chemical compositions of these three types of very high-grade metamorphic rocks were analyzed using the energy dispersive electron microprobe system of JEOL JSM-5310S with JED-2100 at the Okayama University, Japan. The data were obtained under conditions of 15 kv accelerating voltage using data processing by Oxide-ZAF correction program. Natural mineral samples (ASTIMEX MINM25–53) were used as standard for the analyses. Representative data are listed in Tables 1 and 2.

3.1. Garnet–clinopyroxene–orthopyroxene granulites

The garnet–clinopyroxene–orthopyroxene granulites are relatively coarse-grained (see below), homogeneous and weakly foliated. These granulites consist mainly of garnet, clinopyroxene, orthopyroxene, quartz and plagioclase with subordinate rutile, ilmenite, apatite and biotite. The significant textural features seen in these granulites are porphyroblasts, symplectites and moats. Major porphyroblasts are garnet ($Alm_{46.7–47.7}$, $Sps_{0–0.02}$, $Prp_{32.5–34.7}$, $Grs_{16.1–19.3}$), clinopyroxene [X_{Mg}: Mg/(Fe + Mg) = 0.71–0.74 in the core and 0.75–0.78 at the rim] and quartz (Fig. 3a), with various grain sizes of 3–5 mm for garnet, 1–7 mm for clinopyroxene and 1–5 mm for quartz. The orthopyroxene (X_{Mg} = 0.53–0.56, 2.2–2.4 wt% Al_2O_3) and plagioclase ($An_{84.1–91.5}$, $Ab_{8.5–14.2}$, Or_0) coexisting assemblage is present only as a symplectite phase. Orthopyroxene moat (nearly the same composition as that of symplectites) occurs along the grain boundary between symplectites and quartz as identified in some of the thin sections. In some samples, complete consumption of garnet produces pod-like orthopyroxene–plagioclase symplectite as a garnet pseudomorph texture (Fig. 3b).

The major inclusion mineral in garnet and clinopyroxene is quartz with minor amount of ilmenite, rutile, apatite and biotite. No inclusions and porphyroblasts of plagioclase can be identified as initial or primary minerals. Fine lamellae of orthopyroxene (X_{Mg} = 0.57–0.58, 3.6–3.8 wt% Al_2O_3) are also found in clinopyroxene porphyroblasts through the microprobe analyses, which would be indicating an exsolution product from pigeonitic pyroxene (inverted pigeonite). It is notable that hydrous mafic minerals, such as hornblende and biotite, as retrograde minerals are completely absent in most of these granulites, with the exception of biotite inclusions in garnet. Hornblende–orthopyroxene–plagioclase and orthopyroxene–plagioclase symplectites are also identified in some parts of these granulites. From the above textural features, the following decompression and cooling reactions can be assumed in order to consume garnet, clinopyroxene and quartz to produce orthopyroxene, plagioclase and/or hornblende:

$$\mathrm{Grt} + \mathrm{Cpx} + \mathrm{Qtz} = \mathrm{Opx} + \mathrm{Pl} \quad (1)$$

$$\mathrm{Opx} + \mathrm{Cpx} + \mathrm{Pl} + \mathrm{Vapor} = \mathrm{Hbl} + \mathrm{Qtz} \quad (2)$$

$$\mathrm{Cpx} + \mathrm{Vapor} = \mathrm{Hbl} + \mathrm{Qtz} \quad (3)$$

Orthopyroxene moats were also formed during the same stage of reaction (1) as the effect of chemical potential variation of SiO_2.

3.2. Sapphirine-bearing garnet–orthopyroxene–cordierite–sillimanite gneiss

The sapphirine-bearing garnet–orthopyroxene–cordierite–sillimanite gneiss is layered, well foliated, magnesium and aluminous metapelite, which mainly contains garnet, orthopyroxene, cordierite, sillimanite, biotite, plagioclase, K-feldspar and quartz with subordinate ilmenite, rutile, zircon and apatite. Sapphirine (X_{Mg} = 0.73–0.74) is found only as anhedral, fine-grained inclusions coexisting with quartz in garnet porphyroblasts (Fig. 3c).

Two types of garnet occur as (i) subhedral to anhedral, relatively coarse-grained (up to 6 mm) garnet (Grt 1: $Alm_{42.1–42.8}$, $Sps_{1.5–2.4}$, $Prp_{53.2–54.1}$, $Grs_{1.2–2.2}$) with biotite and quartz

Table 1
Representative microprobe analyses for mafic granulite and magnesian-aluminous pelitic gneiss

Rock type	Grt–Cpx–Opx granulite							Spr-bearing Grt–Opx–Crd–Sil gneiss											
Mineral	Grt Core	Grt Rim	Cpx Core	Cpx Rim	Opx sy-(Pl)	Opx Moat	Opx lm-(Cpx)	Spr incl-(Grt)	Grt Coarse	Grt Fine	Opx pb-core	Opx incl-(Grt)	Opx pb-rim	Opx sy-(Sil)	Opx sy-(Crd)	Opx sy-(Spl)	Crd sy-(Opx)	Spl sy-(Opx)	Bt
SiO_2	39.20	39.49	51.52	51.30	50.93	51.00	51.15	16.70	40.45	40.45	47.52	47.31	48.82	49.56	50.00	51.50	49.78	0.00	38.40
TiO_2	0.00	0.00	0.70	0.70	0.00	0.70	0.00	0.10	0.00	0.00	0.50	0.10	0.40	0.00	0.00	0.00	0.00	0.05	4.30
Al_2O_3	22.18	22.30	3.70	4.10	2.40	2.40	3.80	56.80	22.85	22.86	12.95	12.82	9.82	8.90	7.90	6.50	33.80	64.70	15.80
Cr_2O_3	0.10	0.00	0.00	0.00	0.00	0.20	0.10	0.00	0.00	0.00	0.30	0.10	0.10	0.00	0.40	0.00	0.00	0.30	0.20
FeO	22.35	22.59	8.70	6.50	26.80	26.80	24.81	10.40	20.72	21.51	15.52	16.10	17.40	17.90	18.50	17.63	2.30	19.30	9.70
MnO	0.40	0.80	0.00	0.00	0.00	0.00	0.00	0.00	0.70	0.81	0.10	0.00	0.10	0.00	0.40	0.30	0.00	0.00	0.30
MgO	9.09	7.83	13.30	12.10	18.41	17.77	18.86	16.80	14.60	14.32	22.12	21.79	23.00	22.85	22.10	24.42	12.00	15.01	17.30
CaO	6.05	7.70	21.40	23.90	0.70	0.80	1.70	0.00	0.60	0.40	0.60	0.90	0.20	0.30	0.40	0.20	0.00	0.00	0.00
Na_2O	0.00	0.00	0.30	0.70	0.20	0.40	0.30	0.00	0.00	0.00	0.30	0.20	0.00	0.10	0.20	0.00	0.05	0.00	0.20
K_2O	0.00	0.00	0.40	0.30	0.00	0.00	0.00	0.00	0.00	0.00	0.00	0.00	0.00	0.00	0.00	0.00	0.00	0.00	10.20
ZnO	–	–	–	–	–	–	–	–	–	–	–	–	–	–	–	–	–	0.20	–
F	–	–	–	–	–	–	–	–	–	–	–	–	–	–	–	–	–	–	0.22
Cl	–	–	–	–	–	–	–	–	–	–	–	–	–	–	–	–	–	–	0.05
F=O	–	–	–	–	–	–	–	–	–	–	–	–	–	–	–	–	–	–	0.09
Cl=O	–	–	–	–	–	–	–	–	–	–	–	–	–	–	–	–	–	–	0.01
Total	99.37	100.71	100.02	99.60	99.44	100.07	100.72	100.80	99.92	100.35	99.91	99.32	99.84	99.61	99.90	100.55	97.93	99.56	96.57
H_2O*	–	–	–	–	–	–	–	–	–	–	–	–	–	–	–	–	–	–	4.03
Total*	–	–	–	–	–	–	–	–	–	–	–	–	–	–	–	–	–	–	100.60
O	12	12	6	6	6	6	6	10	12	12	6	6	6	6	6	6	18	4	22
Si	3.000	3.001	1.918	1.914	1.948	1.941	1.917	0.996	3.003	3.001	1.718	1.724	1.777	1.810	1.831	1.860	5.001	0.000	5.547
Ti	0.000	0.000	0.020	0.020	0.000	0.020	0.000	0.004	0.000	0.000	0.014	0.003	0.011	0.000	0.000	0.000	0.000	0.001	0.467
Al	2.001	1.998	0.162	0.180	0.108	0.108	0.168	3.992	2.000	1.999	0.552	0.551	0.421	0.383	0.341	0.277	4.002	1.988	2.690
Cr	0.006	0.000	0.000	0.000	0.000	0.006	0.003	0.000	0.000	0.000	0.009	0.003	0.003	0.000	0.012	0.000	0.000	0.006	0.023
Fe	1.431	1.436	0.271	0.203	0.857	0.853	0.778	0.519	1.287	1.334	0.469	0.491	0.530	0.547	0.567	0.533	0.193	0.421	1.172
Mn	0.026	0.051	0.000	0.000	0.000	0.000	0.000	0.000	0.044	0.051	0.003	0.000	0.003	0.000	0.012	0.009	0.000	0.000	0.037
Mg	1.037	0.887	0.738	0.673	1.049	1.008	1.053	1.493	1.616	1.583	1.191	1.183	1.248	1.244	1.206	1.315	1.797	0.583	3.726
Ca	0.496	0.627	0.853	0.955	0.029	0.033	0.068	0.000	0.048	0.032	0.023	0.035	0.008	0.012	0.016	0.008	0.000	0.000	0.000
Na	0.000	0.000	0.022	0.051	0.015	0.030	0.022	0.000	0.000	0.000	0.021	0.014	0.000	0.007	0.014	0.000	0.010	0.000	0.056
K	0.000	0.000	0.019	0.014	0.000	0.000	0.000	0.000	0.000	0.000	0.000	0.000	0.000	0.000	0.000	0.000	0.000	0.000	1.880
Zn	–	–	–	–	–	–	–	–	–	–	–	–	–	–	–	–	–	0.004	–
Total cation	7.996	8.000	4.002	4.009	4.006	3.997	4.009	7.004	7.997	8.000	3.999	4.004	4.000	4.002	3.999	4.001	11.003	2.998	15.597
F	–	–	–	–	–	–	–	–	–	–	–	–	–	–	–	–	–	–	0.100
Cl	–	–	–	–	–	–	–	–	–	–	–	–	–	–	–	–	–	–	0.012
Alm	0.479	0.478	–	–	–	–	–	–	0.430	0.445	–	–	–	–	–	–	–	–	–
Spe	0.009	0.017	–	–	–	–	–	–	0.015	0.017	–	–	–	–	–	–	–	–	–
Pyr	0.347	0.296	–	–	–	–	–	–	0.540	0.528	–	–	–	–	–	–	–	–	–
Grs	0.166	0.208	–	–	–	–	–	–	0.016	0.010	–	–	–	–	–	–	–	–	–
Adr	0.000	0.001	–	–	–	–	–	–	0.000	0.000	–	–	–	–	–	–	–	–	–
Fe^{3+}	–	–	–	–	–	–	–	–	–	–	–	–	–	–	–	–	–	0.005	–
Fe^{2+}	–	–	–	–	–	–	–	–	–	–	–	–	–	–	–	–	–	0.416	–
X_{mg}	0.420	0.382	0.731	0.768	0.550	0.542	0.575	0.742	0.557	0.543	0.717	0.707	0.702	0.695	0.680	0.712	0.903	0.581	0.761
X_f	–	–	–	–	–	–	–	–	–	–	–	–	–	–	–	–	–	–	0.025

Mineral abbreviations are after Kretz (1983). Sy-, synplectite composed with mineral in parenthesis; Im-, lamellae in mineral in parenthesis; pb-, porphyroblast; incl-, inclusion in mineral in parenthesis. H_2O*, calculated according to stoichiometry; Total*, total including calculated H_2O value; XF=F/XF=F/(F+OH+Cl).

Table 2
Representative microprobe analyses for magnesian-aluminous pelitic granulite and aluminous quartzofeldspathic gneiss

Rock type	Spr–Grt–Opx granulite												Crn–Grt–Sil–Spl gneiss						
Mineral	Spr 1 Core	Spr 2 Core	Opx 1 Core	Opx 1 sy-(Spr)	Opx 2 Core	Grt 1 Core	Phl 1 Core	Crd 1 Core	Crd 2 Core	Spl 1 Core	Spl 2 Core	Krn 1 Core	Grt Core	Grt sy-(Spl)	Spl incl-(Grt)	Spl sy-(Sil)	Crn Core	Bt Core	Ky incl-(Grt)
SiO_2	13.39	14.48	52.28	52.95	55.26	40.94	36.61	50.20	50.45	0.00	0.00	29.04	38.62	38.45	0.00	0.00	0.00	38.30	37.51
TiO_2	0.00	0.14	0.17	0.11	0.05	0.01	4.55	0.00	0.02	0.00	0.00	0.22	0.00	0.00	0.00	0.00	0.00	4.69	0.00
Al_2O_3	62.64	61.36	7.79	5.12	5.04	23.17	15.59	34.15	33.24	64.97	66.92	45.57	21.86	21.74	61.21	60.22	98.55	16.18	61.09
Cr_2O_3	0.21	0.14	0.06	0.00	0.00	0.00	0.00	0.00	0.00	0.09	0.07	0.00	0.00	0.00	0.34	0.60	0.14	0.00	0.00
FeO	6.29	3.49	11.08	12.90	6.63	17.01	6.94	2.30	0.87	18.47	10.01	6.30	29.24	28.13	28.69	32.31	1.12	14.21	0.98
MnO	0.21	0.05	0.26	0.47	0.00	1.10	0.00	0.00	0.00	0.00	0.08	0.00	0.76	0.79	0.08	0.19	0.00	0.05	0.00
MgO	16.70	19.59	28.31	28.02	33.64	16.08	20.35	12.20	13.12	14.98	22.23	18.36	7.14	8.09	9.17	5.84	0.00	13.78	0.00
CaO	0.00	0.00	0.06	0.04	0.14	1.97	0.00	0.00	0.01	0.00	0.00	0.00	2.55	2.00	0.00	0.00	0.00	0.16	0.00
Na_2O	0.00	0.00	0.00	0.00	0.00	0.00	0.04	0.00	0.00	0.00	0.00	0.00	0.00	0.00	0.00	0.00	0.00	0.00	0.00
K_2O	0.00	0.00	0.00	0.00	0.00	0.00	9.82	0.00	0.02	0.00	0.00	0.00	0.00	0.00	0.00	0.00	0.00	10.44	0.00
ZnO	–	–	–	–	–	–	–	–	–	0.89	0.20	–	–	–	1.14	0.23	–	–	–
F	–	–	–	–	–	–	1.79	–	–	–	–	–	–	–	–	–	–	0.00	–
Cl	–	–	–	–	–	–	0.00	–	–	–	–	–	–	–	–	–	–	0.25	–
F=O	–	–	–	–	–	–	0.75	–	–	–	–	–	–	–	–	–	–	0.00	–
Cl=O	–	–	–	–	–	–	0.00	–	–	–	–	–	–	–	–	–	–	0.06	–
Total	99.44	99.25	100.01	99.61	100.76	100.28	94.49	98.88	97.73	99.40	99.51	99.49	100.17	99.20	100.63	99.39	99.81	98.00	99.58
H_2O*	–	–	–	–	–	–	3.24	–	–	–	–	–	–	–	–	–	–	4.07	–
Total*	–	–	–	–	–	–	98.18	–	–	–	–	–	–	–	–	–	–	102.07	–
O	10	10	6	6	6	12	6	18	18	4	4	21.5	12	12	4	4	3	22	5
Si	0.797	0.852	1.841	1.890	1.891	2.994	5.367	4.997	5.045	0.000	0.000	3.638	3.002	3.001	0.000	0.000	0.000	5.560	1.020
Ti	0.000	0.006	0.005	0.003	0.001	0.001	0.502	0.000	0.002	0.000	0.000	0.021	0.000	0.000	0.000	0.000	0.000	0.512	0.000
Al	4.392	4.255	0.323	0.215	0.203	1.997	2.693	4.004	3.918	1.997	1.971	6.729	2.003	2.000	1.961	1.982	1.987	2.768	1.958
Cr	0.010	0.007	0.002	0.000	0.000	0.000	0.000	0.000	0.000	0.002	0.001	0.000	0.000	0.000	0.007	0.013	0.002	0.000	0.000
Fe	0.313	0.172	0.326	0.385	0.190	1.040	0.851	0.191	0.073	0.403	0.209	0.660	1.901	1.836	0.652	0.755	0.016	1.725	0.022
Mn	0.011	0.002	0.008	0.014	0.000	0.068	0.000	0.000	0.000	0.000	0.002	0.000	0.050	0.052	0.002	0.004	0.000	0.006	0.000
Mg	1.481	1.718	1.486	1.490	1.716	1.752	4.448	1.809	1.955	0.582	0.828	3.428	0.827	0.941	0.371	0.243	0.000	2.982	0.000
Ca	0.000	0.000	0.002	0.002	0.005	0.154	0.000	0.000	0.001	0.000	0.000	0.000	0.212	0.167	0.000	0.000	0.000	0.025	0.000
Na	0.000	0.000	0.000	0.000	0.000	0.000	0.011	0.000	0.000	0.000	0.000	0.000	0.000	0.000	0.000	0.000	0.000	0.000	0.000
K	0.000	0.000	0.000	0.000	0.000	0.000	1.836	0.000	0.003	0.000	0.000	0.000	0.000	0.000	0.000	0.000	0.000	1.933	0.000
Zn	–	–	–	–	–	–	–	–	–	0.017	0.004	–	–	–	0.023	0.005	–	–	–
Total cation	7.003	7.011	3.992	3.999	4.006	8.007	15.708	11.001	10.996	3.001	3.010	14.476	7.996	7.999	3.016	3.002	2.005	15.511	3.001
F	–	–	–	–	–	–	0.830	–	–	–	–	–	–	–	–	–	–	0.000	–
Cl	–	–	–	–	–	–	0.000	–	–	–	–	–	–	–	–	–	–	0.062	–
Alm	–	–	–	–	–	0.343	–	–	–	–	–	–	0.636	0.613	–	–	–	–	–
Spe	–	–	–	–	–	0.023	–	–	–	–	–	–	0.017	0.017	–	–	–	–	–
Pyr	–	–	–	–	–	0.583	–	–	–	–	–	–	0.277	0.314	–	–	–	–	–
Grs	–	–	–	–	–	0.047	–	–	–	–	–	–	0.071	0.056	–	–	–	–	–
Adr	–	–	–	–	–	0.004	–	–	–	–	–	–	0.000	0.000	–	–	–	–	–
Fe^{3+}	–	–	–	–	–	–	–	–	–	0.001	0.028	–	–	–	0.032	0.005	–	–	–
Fe^{2+}	–	–	–	–	–	–	–	–	–	0.401	0.181	–	–	–	0.620	0.750	–	–	–
X_{mg}	0.826	0.909	0.820	0.795	0.900	0.628	0.839	0.904	0.964	0.591	0.798	0.839	0.303	0.339	0.363	0.244	–	0.634	–
X_f	–	–	–	–	–	–	0.207	–	–	–	–	–	–	–	–	–	–	0.000	–

Mineral abbreviations are after Kretz (1983). Mineral name with numbers 1 and 2 show the domain names in sapphirine–garnet–orthopyroxene granulite. sy-, symplectite composed with mineral in parenthesis; incl-, inclusion in mineral in parenthesis.

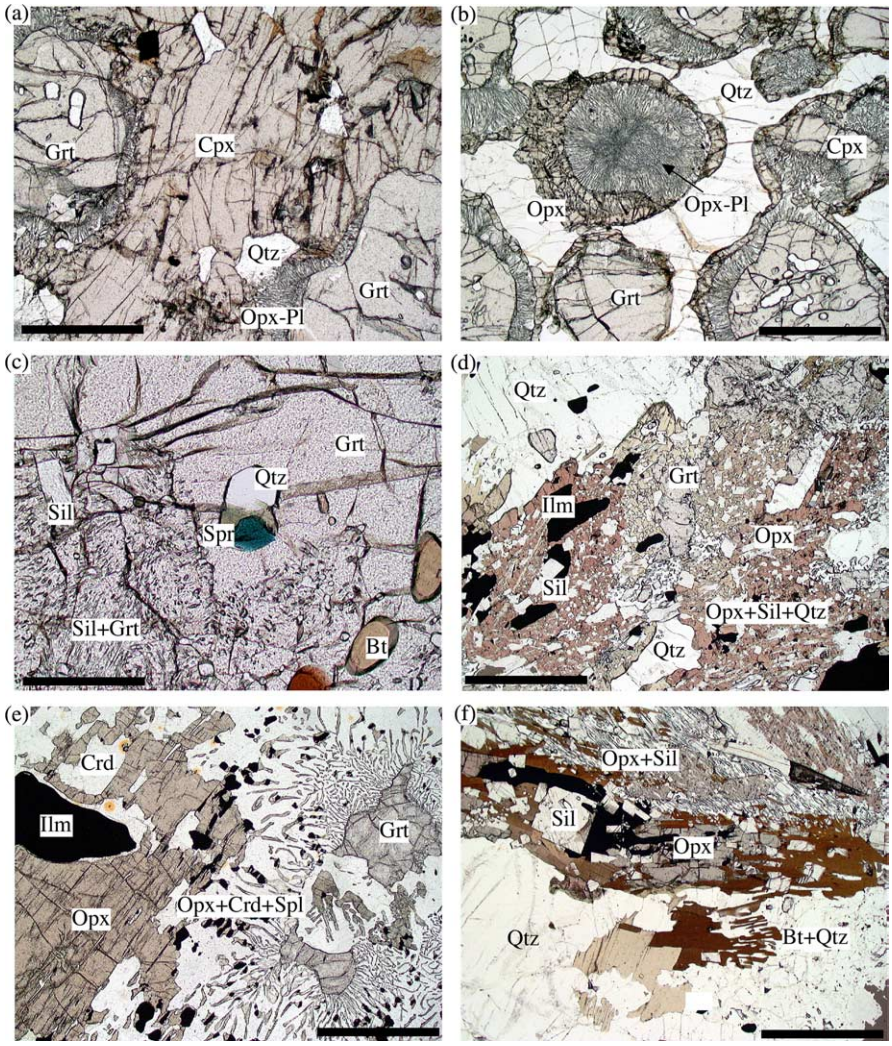

Fig. 3. Photomicrographs of ultrahigh-temperature metamorphic rocks from the Highlamd Complex. (a) and (b): mafic granulite, (c–f): magnesian and aluminous pelitic gneiss (sapphirine-bearing garnet–orthopyroxene–sillimanite gneiss), (g–j) magnesian and aluminous pelitic granulite (sapphirine–garnet–orthopyroxene granulite), (k–n): aluminous quartzofeldspathic gneiss. (a) mafic granulite containing garnet, clinopyroxene and quartz porphyroblasts with thin reaction rim of orthopyroxene–plagioclase symplectite, (b) garnet pseudomorph replaced by orthopyroxene–plagioclase intergrowth, which surrounded by orthopyroxene moat, (c) sapphirine and quartz inclusions in the core of garnet. Euhedral sillimanite and anhedral biotite are also included in garnet rim part, (d) orthopyroxene–sillimanite–quartz intergrowth surrounding anhedral garnet porphyroblast, (e) orthopyroxene–cordierite–spinel symplectite after garnet, (f) retrograde biotite replacing orthopyroxene porphyroblast, (g) sapphirine–garnet–orthopyroxene coexistence in domain 1, (h) garnet porphyroblast rimmed by sapphirine-low-aluminous orthopyroxene–cordierite and low-aluminous orthopyroxene–spinel symplectites, (i) sapphirine–orthopyroxene–cordierite coexistence replaced by later kornerupine, (j) sapphirine–orthopyroxene–quartz coexistence with high-fluorine phlogopite, (k) garnet–corundum–quartz coexistence, (l) backscattered SEM-image of kyanite inclusion in garnet porphyroblast, (m) fine-grained sillimanite–spinel intergrowths surrounding garnet and garnet–corundum coexistence, (n) backscattered SEM-image of magnetite exsolution lamellae in spinel. Scale bar indicates 1 mm in each photomicrograph excepting (c): 0.5 mm, (l): 100 μm, (n): 50 μm.

inclusions and (ii) subhedral, elongated, fine-grained (up to 3 mm) garnet (Grt 2: $Alm_{44.5–49.8}$, $Sps_{1.3–2.5}$, $Prp_{48.2–53.3}$, $Grs_{1.1–2.1}$) with sillimanite (fibrolite). The former type, which also includes sapphirine, is generally associated with orthopyroxene–sillimanite–quartz and is sometimes rimmed by orthopyroxene–cordierite symplectite at the boundary between garnet and quartz. The latter type of garnet occurs only in cordierite-dominant domain or band (up to 10 mm thick).

Orthopyroxene occurs as inclusion in garnet (Grt 1), coarse- or fine-grained porphyroblasts and as symplectite phases. Core compositions of coarse-grained orthopyroxene (up to 8 mm) and inclusions in garnet have the highest aluminum content (X_{Mg} = 0.69–0.72, 11.6–13.0 wt% Al_2O_3: Fig. 4). Fine-grained orthopyroxene porphyroblasts (up to 2 mm) as well as rim of coarse orthopyroxene have a less Al_2O_3 content (X_{Mg} = 0.67–0.72, 9.7–9.8 wt% Al_2O_3). Orthopyroxene (X_{Mg} = 0.67–0.74, 8.8–8.9 wt% Al_2O_3) coexisting with sillimanite and quartz (sometimes forming symplectite) occurs as anhedral grains of varying sizes (0.5–7 mm) showing a marked pleochroism (Fig. 3d). In some portions, orthopyroxene (X_{Mg} = 0.67–0.72, 7.9–8.2 wt% Al_2O_3)-cordierite (X_{Mg} = 0.88–0.93) and orthopyroxene (X_{Mg} = 0.69–0.74, 6.5–7.2 wt% Al_2O_3)-spinel (X_{Mg} = 0.57–0.61) intergrowths are also identified surrounding garnet

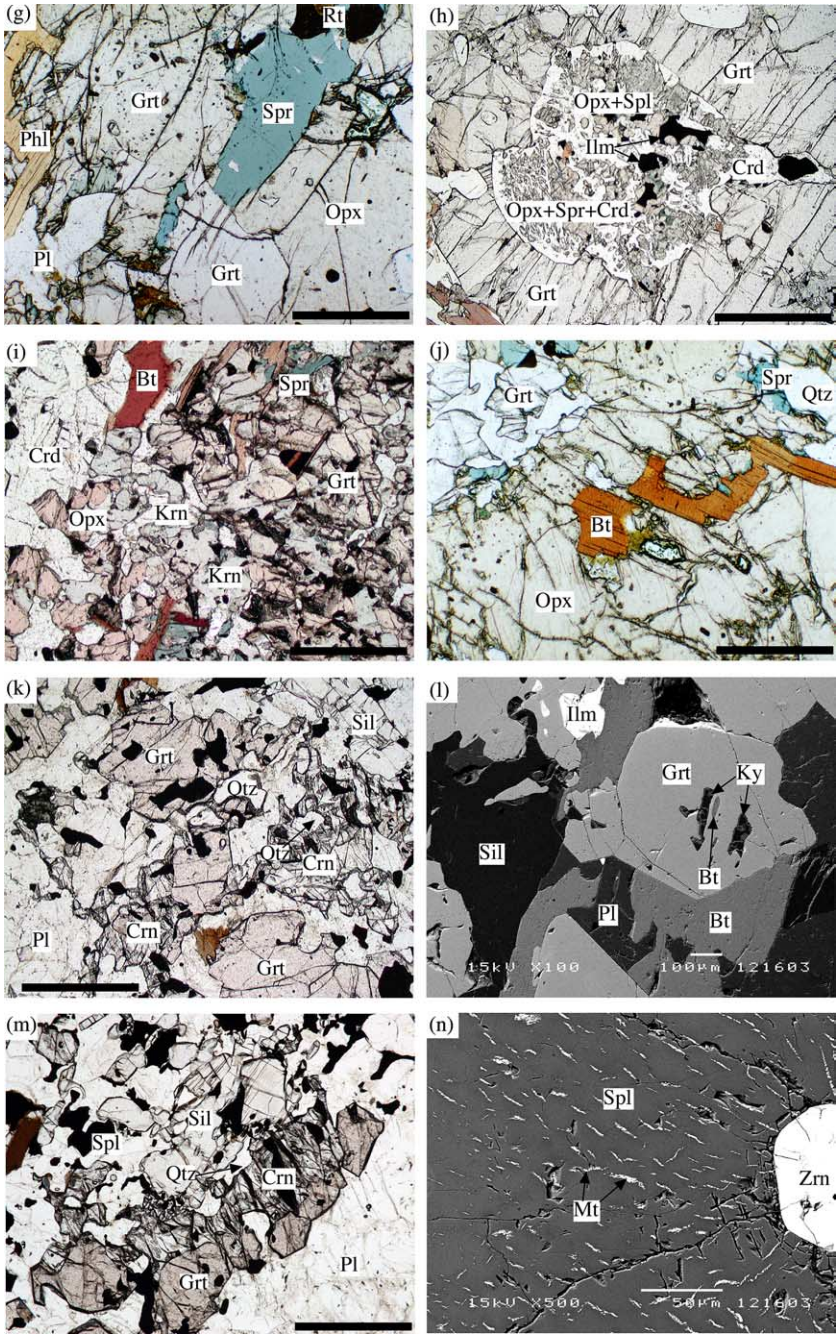

Fig. 3 (*continued*)

(Fig. 3e). Low-fluorine biotite [X_{Mg} = 0.75–0.78, F/(F + OH + Cl = 0.0–0.03)] occurs as an euhedral to subhedral, fine to coarse-grained retrograde mineral phase overprinting garnet, orthopyroxene, cordierite and symplectites containing these minerals. These textural relationships suggest the following reactions:

$$\mathrm{Spr} + \mathrm{Qtz} = \mathrm{Grt1} + \mathrm{Sil} \quad (4)$$

$$\mathrm{Grt1} + \mathrm{Spr} + \mathrm{Qtz} = \mathrm{Opx} + \mathrm{Sil} \quad (5)$$

$$\mathrm{Opx} + \mathrm{Sil} + \mathrm{Qtz} = \mathrm{Grt2} + \mathrm{Crd} \quad (6)$$

$$\mathrm{Grt1} + \mathrm{Spr} = \mathrm{Opx} + \mathrm{Crd} + \mathrm{Spl} \quad (7)$$

$$\mathrm{Grt} + \mathrm{Qtz} = \mathrm{Opx} + \mathrm{Crd} \pm \mathrm{Pl} \quad (8)$$

The rare occurrence of comb-like biotite–quartz intergrowth replacing orthopyroxene and garnet would be indicating a vapor-present cooling reaction texture (Fig. 3f) by the following reactions:

$$\mathrm{Opx} + \mathrm{Vapor} = \mathrm{Bt} + \mathrm{Qtz} \quad (9)$$

$$\mathrm{Grt} + \mathrm{Vapor} = \mathrm{Bt} + \mathrm{Qtz} \quad (10)$$

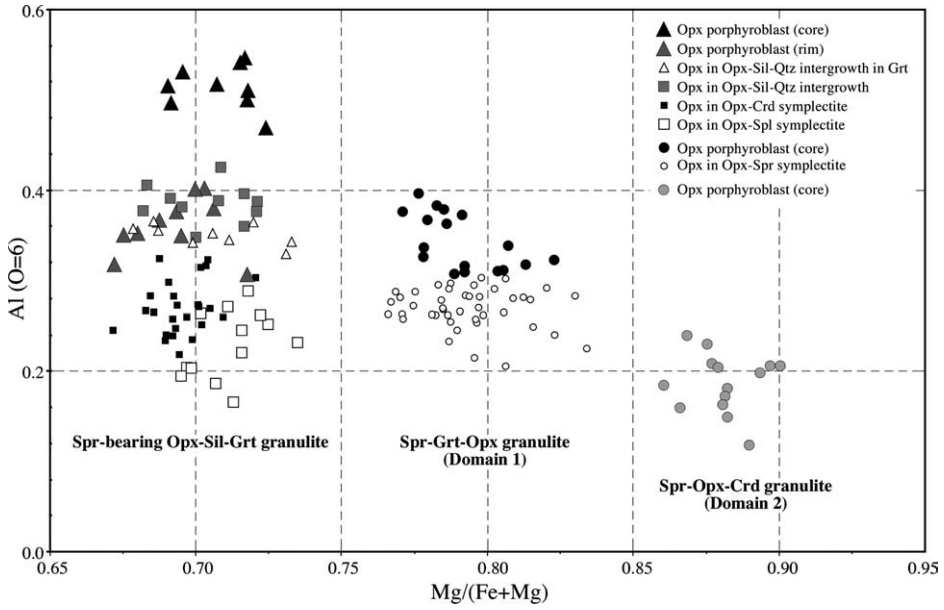

Fig. 4. Chemical compositions of orthopyroxene from magnesian and aluminous pelitic metamorphic rocks.

3.3. Sapphirine–garnet–orthopyroxene granulite

The sapphirine–garnet–orthopyroxene granulites are layered, poorly foliated, silica-poor and magnesium and aluminous metapelites containing sapphirine, orthopyroxene, garnet, spinel, kornerupine, cordierite, sillimanite, gedrite, phlogopite/biotite, and plagioclase (Fig. 3g). Minor constituents are quartz, K-feldspar, ilmenite, rutile, pyrrohtite, pyrite, magnesite, apatite and zircon. These mineral contents were described from a series of samples as no single sample contains the full set of these minerals.

Based on their mineral assemblages, the granulites can be divided into two microdomains (max. 30 cm in diameter) for the petrographic descriptions, which appear to have equilibrated at different fO_2 conditions (Osanai et al., 2000). Domain 1 characteristically contains garnet and highly unusual, euhedral, oscillatory-zoned plagioclase coexisting with sapphirine ($X_{Mg}=0.77$–0.86)-orthopyroxene ($X_{Mg}=0.76$–0.83)-garnet ($Alm_{37.9–48.8}$, $Sps_{0.1–3.9}$, $Prp_{41.7–54.3}$, $Grs_{4.7–7.7}$)-phlogopite ($X_{Mg}=0.75$–0.91) ± cordierite ($X_{Mg}=0.88$–0.90) ± spinel ($X_{Mg}=0.59$–0.63, $Fe^{3+}/Fe^{2+}=0.0$–0.05) ± kornerupine ($X_{Mg}=0.73$–0.88). Quartz occurs only as inclusion in garnet and orthopyroxene. Ilmenite and rutile are also present. Domain 2 is characterized by the appearance of quartz, the predominance of spinel and the rare occurrence of garnet [sapphirine ($X_{Mg}=0.89$–0.91)-orthopyroxene ($X_{Mg}=0.86$–0.90)-quartz–spinel ($X_{Mg}=0.72$–0.81, $Fe^{3+}/Fe^{2+}=0.13$–0.21)-cordierite ($X_{Mg}=0.94$–0.96)-garnet ($Alm_{34.4–36.6}$, $Sps_{0.6–2.4}$, $Prp_{56.1–58.2}$, $Grs_{4.8–7.2}$)-gedrite ± phlogopite ± sillimanite].

In domain 1, high-fluorine phlogopite [F/(F + Cl + OH) = 0.10.3] and quartz inclusions in porphyroblastic orthopyroxene (up to 1.2 cm), and fine-grained garnet inclusions in oscillatory-zoned plagioclase indicate prograde metamorphism and/or a phlogopite-consuming melting reaction, which involves phlogopite, quartz and garnet. Sapphirine, relatively high-aluminous orthopyroxene (7.4–9.0 wt% Al_2O_3) and garnet coexist, often rimmed by a symplectites of sapphirine, low-aluminous orthopyroxene (4.5–6.2 wt% Al_2O_3) and cordierite or low-aluminous orthopyroxene (5.7–6.2 wt% Al_2O_3) and spinel (Fig. 3h). The kornerupine–orthopyroxene ± biotite assemblage is believed to have formed during retrograde metamorphism at the expense of garnet and sapphirine (Fig. 3i). In domain 2, sapphirine, orthopyroxene, quartz and minor K-feldspar are coexisting as the peak metamorphic assemblage (Fig. 3j). Absence or rare occurrence of sillimanite would indicate consumption of sillimanite in forming sapphirine–cordierite and sapphirine–cordierite–plagioclase symplectites. These textures suggest the following reactions during retrograde process:

$$\text{Grt} + \text{high} - \text{F Phl} + \text{Qtz} = \text{Opx} + \text{melt(Pl} + \text{Kfs} \pm \text{Qtz)} \quad (11)$$

$$\text{Grt} = \text{Spr} + \text{low} - \text{Al Opx} + \text{Crd} \quad (12)$$

$$\text{Spr} + \text{high} - \text{Al Opx} = \text{Spl} + \text{low} - \text{Al Opx} \quad (13)$$

$$\text{Opx} + \text{Sil} = \text{Spr} + \text{Crd} \pm \text{Grt} \quad (14)$$

$$\text{Grt} + \text{Sil} = \text{Spr} + \text{Crd} \pm \text{Pl} \quad (15)$$

$$\text{Spr} + \text{Opx} + \text{Crd} + \text{Vapor} = \text{Krn} \quad (16)$$

These reactions indicate that domain 1 equilibrated under relatively low-fO_2 condition, whereas fO_2 was higher in domain 2 (Osanai et al., 2000).

3.4. Corundum–garnet–sillimanite–spinel gneiss

The aluminous quartzo-feldspathic corundum–garnet–sillimanite–spinel gneiss is relatively fine grained, well foliated melanocratic rock containing garnet, sillimanite, corundum, spinel, plagioclase, and quartz. Minor constituents are ilmenite, magnetite, zircon, apatite, biotite and kyanite. Garnet–corundum–sillimanite, garnet–sillimanite–spinel and rare garnet–corundum–quartz coexisting assemblages are identified even in a single sample, although no spinel–quartz direct contact is observed (Fig. 3k).

Garnet ($Alm_{63.6–68.5}$, $Sps_{1.3–2.4}$, $Prp_{23.2–27.7}$, $Grs_{5.4–8.5}$) occurs as subhedral porphyroblasts up to 7 mm in diameter. Inclusions of spinel, ilmenite and quartz are common in garnet and rare kyanite inclusions also occur in garnet (Fig. 3l). In the core of garnet, micro domains of garnet ($Alm_{61.4–64.0}$, $Sps_{0.7–1.8}$, $Prp_{27.8–31.4}$, $Grs_{4.2–6.1}$)-spinel ($X_{Mg}=0.30–0.36$) symplectites are also observed. Fine-grained (up to 2 mm) sillimanite-spinel ($X_{Mg}=0.21–0.28$) intergrowths occasionally surround the garnet or garnet–corundum coexistence (Fig. 3m). These textures not only suggest the following reactions but also that the host gneiss had passed through the kyanite stability field:

$$Crn + Qtz = Sil \quad (17)$$

$$Grt + Crn = Sil + Spl \quad (18)$$

These reactions would have taken place under high-fO_2 condition, which is explained by the occurrence of magnetite–spinel coexistence and magnetite exsolution in spinel (Fig. 3n).

4. Metamorphic evolution of the highest-grade metamorphic rocks

Reaction textures and mineral chemical features of the high-grade metamorphic rocks from the Highland Complex, as described above, are useful to determine their metamorphic evolution processes. Some petrogenetic grids and geothermobarometric calibrations are used for the estimation of pressure–temperature (P–T) paths.

4.1. P–T path and metamorphic conditions of mafic granulites

Metamorphic temperature for the orthopyroxene- and plagioclase-absent initial assemblage is estimated by using the garnet–clinopyroxene Fe–Mg exchange geothermometers for representative core compositions. For the pressure condition, it is estimated by the reaction *orthopyroxene + plagioclase = garnet + clinopyroxene + quartz*, which is equivalent to the reverse of the above mentioned reaction (1), through the experimental results of basalt compositions (Green and Ringwood, 1967). From their results, 'garnet-in' and 'plagioclase-out' reactions have been determined, and three different fields have been recognized as 'orthopyroxene–clinopyroxene–plagioclase', 'garnet–orthopyroxene–clinopyroxene–plagioclase' and 'garnet–clinopyroxene–quartz', which depend on P–T conditions as well as the bulk chemical compositions of 'quartz tholeiite' or 'olivine tholeiite' (Fig. 5).

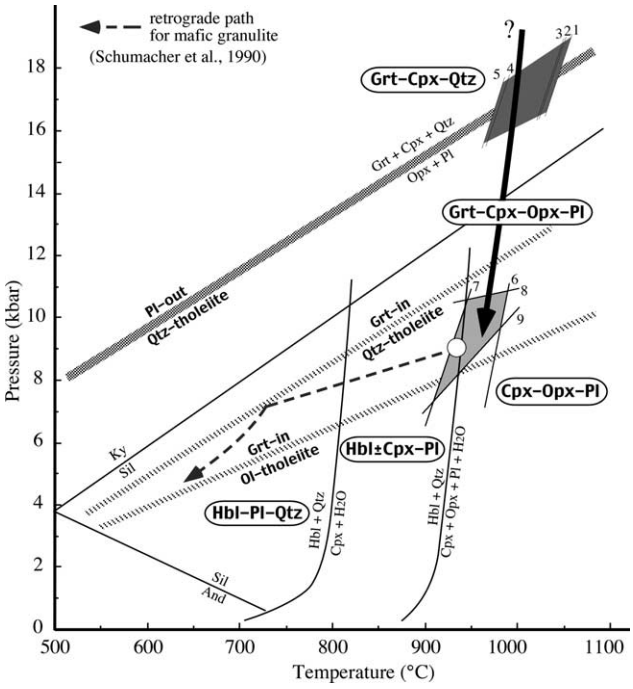

Fig. 5. Inferred P–T path and estimated metamorphic conditions of garnet–clinopyroxene–orthopyroxene granulite from the central Highland Complex. Geothermobarometers used here are as follows; (1) Ellis and Green (1979), (2) Powell (1985), (3) Krogh (1988), (4) Ai (1994), (5) Krogh (2000), (6) Lee and Ganguly (1988), (7 and 8) Bhattacharya et al. (1991), (9) Harley and Green (1982). Plagioclase-out and garnet-in lines are after Green and Ringwood (1967). Hornblende producing univariant reactions are from Spear (1993).

To estimate the highest-pressure condition, we consider the reactions involving quartz tholeiitic composition, because the bulk chemical compositions of garnet–clinopyroxene–orthopyroxene granulites studied here have a quartz tholeiitic affinity with quartz-normative characteristics. We also consider the garnet–orthopyroxene exchange thermometer for the rim composition of garnet and orthopyroxene moats to estimate retrograde conditions. The retrograde pressure is also calibrated by using garnet–orthopyroxene–plagioclase–quartz net-transfer reaction barometry.

Temperature calibration using core compositions of coexisting garnet–clinopyroxene pairs gives a maximum temperature of 1035 °C by the method of Ellis and Green (1979), which indicates the highest value at pressure of 17 kbar as mentioned below. The geothermometric methods suggested by Powell (1985) and Krogh (1988) also give similar temperatures of c. 1020 °C. The calibrations using the methods of Ai (1999) and Krogh (2000) indicate slightly lower temperatures of 975 and 970 °C, respectively, at the same pressure. The pressure for the orthopyroxene- and plagioclase-free initial assemblage is determined to be above 17 kbar as a maximum pressure condition using these temperatures, which is equivalent to the 'plagioclase-out' field in the P–T space (Fig. 5). Calibrations using garnet-rim and orthopyroxene-moat for garnet–orthopyroxene exchange thermometer by Lee and Ganguly (1988) give the retrograde temperature of 982 °C, while that of Bhattacharya et al. (1991) is 938 °C at 10 kbar. Lower temperature of 875 °C is also calibrated by the method

of Lal (1993). The retrograde pressures are calculated using rim compositions of coexisting garnet–orthopyroxene–plagioclase–quartz (GOPS) and also using garnet—orthopyroxene pairs. Methods by Harley and Green (1982) and Wood (1974) indicate pressures of 10.8 and 10.5 kbar, respectively. Results from the barometer by Bhattacharaya et al. (1991) give a higher value of c.11 kbar. The GOPS barometer by Newton and Perkins (1982) shows a pressure between 9.1 and 10.7 kbar, while that of Bohlen et al. (1983) gives the lowest value of 8.5–9.5 kbar.

The estimated retrograde pressures are certainly lower than the pressure determined for the initial assemblages. But the temperatures estimates for both initial and retrograde assemblages are nearly the same, which can be interpreted that the P–T path would indicate a near isothermal decompression (Fig. 5). This isothermal decompression path indicates the ultrahigh-temperature metamorphism even in the retrograde conditions. The estimated retrograde P–T conditions show nearly the same values to the starting point of the retrograde P–T path down to more low-temperature–pressure side of Schenk et al. (1988) and Schumacher et al. (1990) for the hornblende-bearing mafic granulites (Fig. 5). During the progressive retrograde process along with their P–T path, hornblende would be formed in the stability field of hornblende (e.g. Spear, 1993), before the mineral reactions were frozen.

4.2. P–T path and metamorphic conditions of magnesium and aluminous pelitic metamorphic rocks

The mineral reactions observed in the very high-grade magnesium and aluminous metamorphic rocks can be interpreted using the petrogenetic grids in the model FMAS and KFMASH systems (e.g. Harley, 1998; McDade and Harley, 2001). On the basis of the petrographic observations described above, the reaction to produce orthopyroxene + sillimanite + quartz intergrowth [reaction (5)] has taken place at the high-pressure side of [Spl, Bt] invariant point, which gives constraints on pressure and nearly isobaric P–T path (Fig. 6). The reactions to produce the garnet + cordierite [reaction (6)] and orthopyroxene + cordierite + spinel [reaction (7)] coexistences in quartz- and sapphirine-bearing garnet–orthopyroxene–cordierite–sillimanite gneisses and sapphirine + cordierite ± garnet ± plagioclase [reactions (14) and (15)] paragenesis in sapphirine–garnet–orthopyroxene granulites give a decompression path between [Spl, Bt]

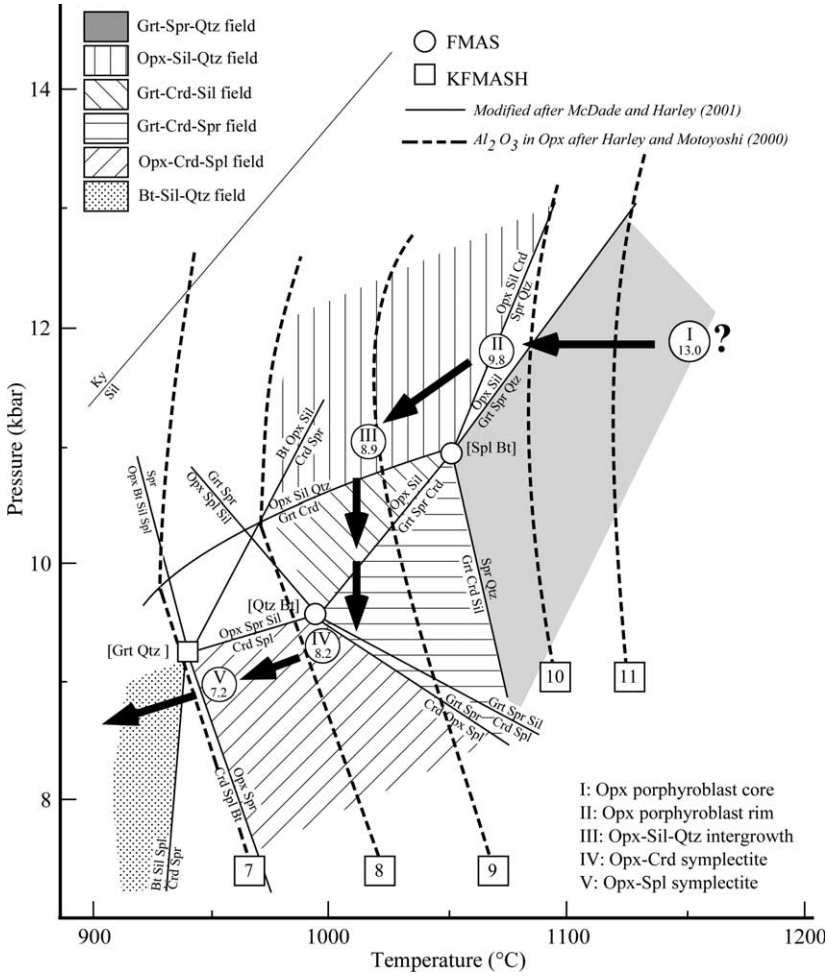

Fig. 6. Inferred P–T path for magnesian and aluminous pelitic gneisses and granulites. Note the alumina content of orthopyroxene in the sapphirine-bearing garnet–orthopyroxene–cordierite–sillimanite gneiss decreases systematically from stage 1 to stage 5 reflecting petrographical textures.

Table 3
Thermobarometric estimation of peak metamorphic condition for sapphirine-bearing garnet–orthopyroxene–sillimanite gneiss

Gartnet		Orthopyroxene		Plagioclase									
X_{Mg}	X_{Grs}	X_{Mg}	X_{Al}	X_{Ca}	*P*(ref.)	K_D	TH84	TLG88	TB91	*T*(ref.)	PHG82	PB91	PW74
0.558	0.022	0.686	0.250	0.286	(11–12)	1.737	1056	1167	1118	(1150)	11.6	9.3	12.5
0.557	0.012	0.690	0.261	0.299	(11–12)	1.769	1039	1140	1099	(1150)	11.6	7.3	12.4
0.557	0.022	0.695	0.271	0.290	(11–12)	1.808	1028	1135	1092	(1150)	11.1	9.9	11.7
0.552	0.020	0.707	0.275	0.266	(11–12)	1.960	945	1039	1005	(1150)	11.3	9.0	11.9
0.550	0.024	0.709	0.216	0.329	(11–12)	1.986	955	1053	1019	(1150)	12.7	9.6	13.7

T(ref.) and *P*(ref.) represent reference temperature and pressure, respectively, for estimation of peak conditions. TH84, Harley (1984); TLG88, Lee and Ganguly (1988); TB91, Bhattacharya et al. (1991); PHG82, Harley and Green (1982); PB91, Bhattacharya et al. (1991); PW74, Wood (1974).

and [Qtz, Bt] invariant points. According to McDade and Harley (2001), the P–T conditions of the invariant points [Spl, Bt] and [Qtz, Bt] in the FMAS system lie around 10.5–11 kbar and 1050 °C and near 9.5 kbar and 980 °C, respectively (Figs. 6 and 8). The biotite-producing reaction [reactions (9) and (10)] in garnet–orthopyroxene–cordierite–sillimanite gneisses would indicate a vapor-present cooling process under pressures below [Qtz, Bt] in the FMAS and [Grt, Qtz] (at c. 9.2 kbar and 940 °C) in KFMASH systems. The konerupine producing reaction [reaction (16)] in sapphirine–garnet–orthopyroxene granulites would have taken place under more low-pressure and -temperature conditions than [Grt, Qtz] invariant point as suggested by Seifert (1975), Droop (1989) and Goscombe (1992).

Metamorphic temperature conditions were estimated using not only some geothermometers but also a chemical isopleth diagram for the Al_2O_3 content in orthopyroxene by Hensen and Harley (1990) and by later revised version of Harley and Motoyoshi (2000). Here, orthopyroxenes from sapphirine-bearing garnet–orthopyroxene–cordierite–sillimanite gneiss are used for determine the metamorphic conditions. As described above, maximum Al_2O_3 content in orthopyroxene is highly variable along with the change in coexisting minerals through the retrograde process. The core of orthopyroxene porphyroblasts coexisting with garnet and orthopyroxene inclusions in garnet have up to about 13.0 wt% Al_2O_3 content (Figs. 4 and 6), which is equivalent to a temperature higher than c. 1120 °C at around 11 kbar (high-pressure side of [Spl, Bt] as described above). Rim composition of the orthopyroxene porphyroblasts shows slightly a low-Al_2O_3 content of 9.8 wt%, which may indicate c. 1050–1100 °C at the same pressure. However, Al_2O_3 contents in orthopyroxene are continuously decreasing from 8.9 wt% (c. 1020 °C at 10.5–11 kbar, just the low-temperature side of [Spl, Bt]) in symplectites composed of sillimanite and quartz to 7.2 wt% (c. 950 °C at 8.5–9 kbar, the low-pressure side of [Grt, Qtz]) in spinel–orthopyroxene symplectites through 8.2 wt% (c. 1000 °C at c. 9.0 kbar, low-pressure side of [Qtz, Bt]) in cordierite–orthopyroxene symplectites.

Geothermobarometric estimations of the peak conditions (Table 3) using core compositions of high-aluminous orthopyroxene, garnet and plagioclase give a wide temperature range of 950–1170 °C (reference pressure is 11–12 kbar) by the methods of Harley (1984), Lee and Ganguly (1988) and Bhattacharya et al. (1991) and a pressure range of 7.3–13.7 kbar (reference temperature is 1150 °C) by the methods of Harley and Green (1982), Bhattacharya et al. (1991) and Wood (1974). Temperature estimations by the methods of Sen and Bhattacharya (1984) and Aranovich and Berman (1997) yield an extremely high temperature of c. 1300–1400 °C and the pressure estimation using Harley (1984)'s method gives a very low values of 6–7.5 kbar. Therefore, the petrogenetic grid and Al_2O_3-isopleth for orthopyroxene are rather useful than geothermobarometries to establish a P–T path and metamorphic conditions through the evolution of magnesium and aluminous pelitic metamorphic rocks.

4.3. P–T path and metamorphic conditions of aluminous quartzo-feldspathic metamorphic rocks

The mineral assemblages observed in aluminous quartzo-feldspathic gneiss can be interpreted using the system FeO–Al_2O_3–SiO_2 petrogenetic grid by Anovitz et al. (1993) and Guiraud et al. (1996) and their compiled diagram by Shaw and Arima (1998) (Fig. 7). Shaw and Arima (1998) suggested the pressure and temperature conditions of two invariant points of [Grt, Spl] and [Ky] in the petrogenetic grid as c. 13.7 kbar and c. 1010 °C and c. 11.8 kbar and c. 1100 °C, respectively, when using the data from Guiraud et al. (1996).

In previous works, thermodynamic equilibrium of the 'corundum + quartz' assemblage was thought possible (Aramaki and Roy, 1963; Krogh, 1977; Guiraud et al., 1996; Shaw and Arima, 1998). However, new thermodynamics datasets suggest that the assemblage is metastable over all crustal conditions (Harlov and Milke, 2002 and references therein). Harlov and Milke (2002) carried out the experimental work on SiO_2–Al_2O_3 system, while Krogh (1977) suggested that a relatively high content of Fe^{3+} in corundum might stabilize corundum + quartz rather than aluminosilicates. Actually, corundum in aluminous quartzo-feldspathic gneiss from the Highland Complex contains relatively high Fe^{3+} (Table 2). On the basis of the natural occurrences of corundum + quartz in the world, reviewed by Mouri et al. (2004), the 'texturally' stable 'corundum + quartz' assemblage observed mainly in the magnetite–ilmenite–spinel bearing high-grade metamorphic rocks is consistent with ultrahigh-temperature and dry conditions. Therefore, we assume that corundum + quartz coexistence in aluminous qurtzo-feldspathic gneiss would be a stable assemblage.

The divariant mineral assemblage of garnet–corundum–quartz would indicate the peak metamorphic condition.

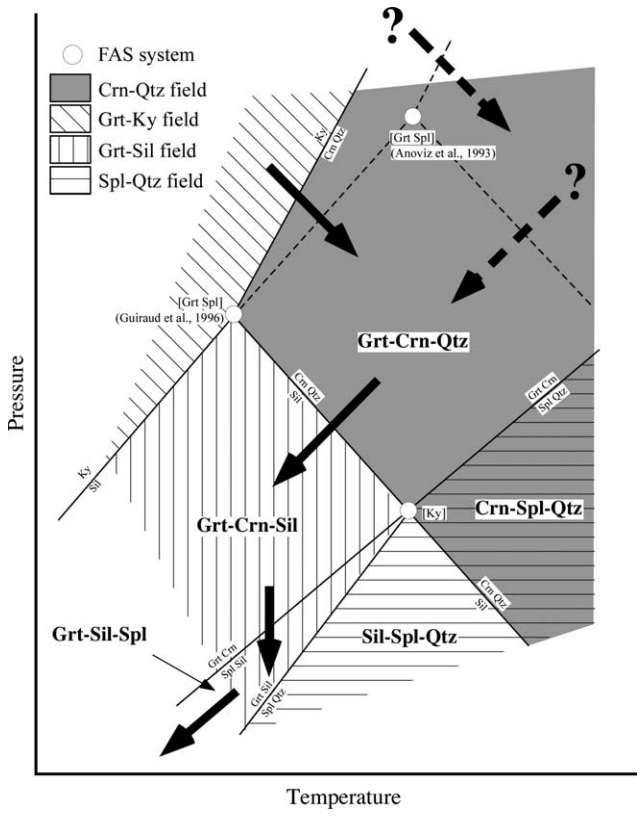

Fig. 7. Inferred P–T path for corundum-bearing aluminous quartzofeldspathic gneiss as a change in divariant assemblages. Petrogenetic grid is modified after Shaw and Arima (1998). Broken arrows show the possible P–T path when using the grid of Anoviz et al. (1993).

Mineral coexistences of garnet–corundum–sillimanite and garnet–sillimanite–spinel would also have formed during the retrograde stage through the presumable mineral reactions of (17) and (18) as described above. The reactions (17) and (18) are rather sensitive to cooling and decompression, respectively (Fig. 7). However, the decompressional process has not extended into the spinel–quartz stability field. The presence of kyanite inclusions in garnet porphyroblasts indicates that the metamorphic pressure was already high enough to be in the kyanite stability field before producing the peak assemblage of garnet–corundum–quartz. Fig. 8 is the combined petrogenetic grid for magnesium and aluminous pelitic and aluminous quartzo-feldspathic metamorphic rocks under ultrahigh-temperature conditions. The possible P–T path is indicated as a single evolution path, which assumes from change in divariant assemblages (shaded areas in Fig. 8) of both metamorphic rock types considering the pressure–temperature conditions of each invariant point, but the highest-pressure condition is not recognized yet through the evolution process (Fig. 8).

5. Discussion and concluding remarks

Metamorphic evolution of three types of ultrahigh-temperature metamorphic rock from the Highland Complex will be discussed here. For a clear understanding of the metamorphic evolution of these rocks, we have used experimentally and theoretically well constrained petrogenetic grids. As described elsewhere, we combined three types of petrogenetic grids for mafic granulite, magnesium and aluminous pelitic granulites and aluminous quartzo-feldspathic granulites (Fig. 9). In general, univariant metamorphic reactions in each grid are very difficult to identify, even though many kinds of divariant mineral assemblages through the metamorphic evolution can be observed. From garnet–clinopyroxene–orthopyroxene granulites (mafic granulite), divariant assemblages of garnet–clinopyroxene–quartz, clinopyroxene–orthopyroxene–plagioclase-(garnet) and hornblende–quartz are identified as a result of their metamorphic evolution (Table 4). The first high-pressure assemblage (at stage 0 in Fig. 9) indicates c.16–17 kbar and c. 950–1050 °C, where estimated pressure would be indicating a maximum condition, and the second assemblage (at stage 4 in Fig. 9) shows the metamorphic conditions at around 9 kbar and 950 °C. Based on observations made in mafic granulites, the simplified connection between these two conditions would be a steep isothermal decompression path (path 1 in Fig. 9), then moving to more low-temperature conditions with hornblende forming for a total P–T path of mafic granulite.

Table 4
Characteristic divariant mineral assemblages of UHT-metamorphic rocks from Highland Complex, Sri Lanka

Stage	Mafic granulite	Mg–Al pelitic gneisses	Qtz-feld. gneiss
0	Grt–Cpx–Qtz	(Opx–Spr–Qtz?)	Grt–Ky–Qtz
1	(Grt-)Cpx–Opx–Pl	Grt1–Spr–Qtz	Grt–Crn–Qtz
2	ditto	Opx–Sil–Qtz	Grt–Sil–Qtz
3	ditto	Grt2–Crd–Opx Grt2–Crd–Spr	Grt–Sil–Spl
4	ditto	Opx–Crd–Spl	ditto
5	Hbl–(Cpx)–Qtz	Bt–Sil–Qtz	ditto

From the magnesium and aluminous pelitic granulites and aluminous quartzo-feldspathic granulites, we are able to observe more complicated divariant assemblages (Table 4) through the P–T path in Fig. 8. The metamorphic peak divariant assemblages (at stage 1 in Fig. 9) for both rock types are garnet–sapphirine–quartz and garnet–corundum–quartz, and the recognized final divariant assemblages are biotite–sillimanite–quartz and garnet–sillimanite–spinel (at stage 5 in Fig. 9). Divariant assemblages at stages 2–4 are also characterized as shown in Table 4. Al-orthopyroxene, sapphirine and quartz inclusions in garnet from magnesium and aluminous pelitic granulite and kyanite inclusions in garnet from corundum-bearing aluminous quartzo-feldspathic granulite are also indicating that the P–T path starts from relatively higher-pressure side, which would be equivalent to the stage 0 derived from mafic granulite.

All three rock types studied here are collected from nearby areas within the central Highland Complex. However, the corundum-bearing aluminous quartzo-feldspathic granulite occurs at a location considerably away from the other locations. Yet, it may be considered that the metamorphic evolution of these three ultrahigh-temperature metamorphic

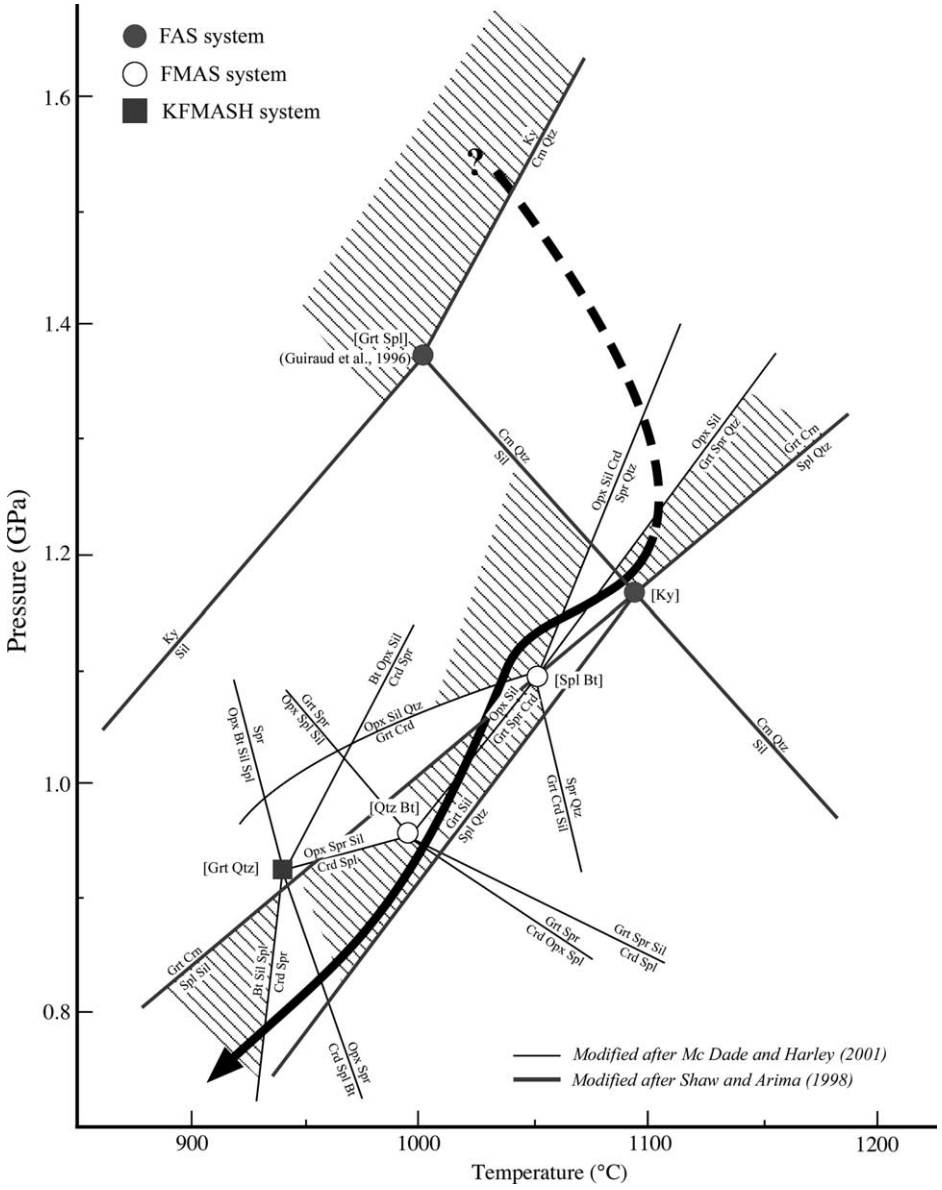

Fig. 8. Combined P–T path for pelitic and quartzofeldspathic gneisses. Shaded areas indicate adequate divariant assemblages for both rock types.

rocks would be the same. Therefore, we may adopt a common P–T path for different lithologies (hence assemblages). If we adopt the path 2 to be common for both mafic granulite, pelitic and quartzo-feldspathic granulites, divariant assemblages for the mafic granulite between immediately after the stage 0 and before the stage 4 would not be changed as clinopyroxene–orthopyroxene–plagioclase–(garnet) (Table 4 and Fig. 9).

It is concluded that ultrahigh-temperature metamorphic rocks from the Highland Complex of Sri Lanka show a clockwise P–T path with the peak metamorphic conditions of ~12 kbar and ~1100 °C (stage 1 in Fig. 9). A high-pressure metamorphism (stage 0 in Fig. 9) as part of the prograde metamorphism and a low-pressure (but still ultrahigh-temperature) metamorphism (stages 2–5 in Fig. 9) as part of the retrograde metamorphism during the clockwise P–T evolution are also identified. These retrograde assemblages from the ultrahigh-temperature metamorphic rocks, especially for stages 3–5, have the same mineral constituents to the surrounding ordinary granulite–facies gneisses. Therefore, there is a possibility that the high-pressure and ultrahigh-temperature metamorphic rocks (assemblages) in the Highland Complex would have been frozen before and remaining after significant retrograde metamorphism as well as deformation and then form boudinaged blocks, lenses and disrupted layers surrounded by ordinary granulites.

Recently, the same situation is also identified for the high-grade metamorphic rocks from Rundvågshetta in the Lützow-Holm Complex, east Antarctica, where sapphirine + quartz- and kyanite-bearing ultrahigh-temperature granulites outcrop as blocks, lenses and disrupted layers surrounded by garnet–orthopyroxene and garnet–cordierite gneisses of ordinary

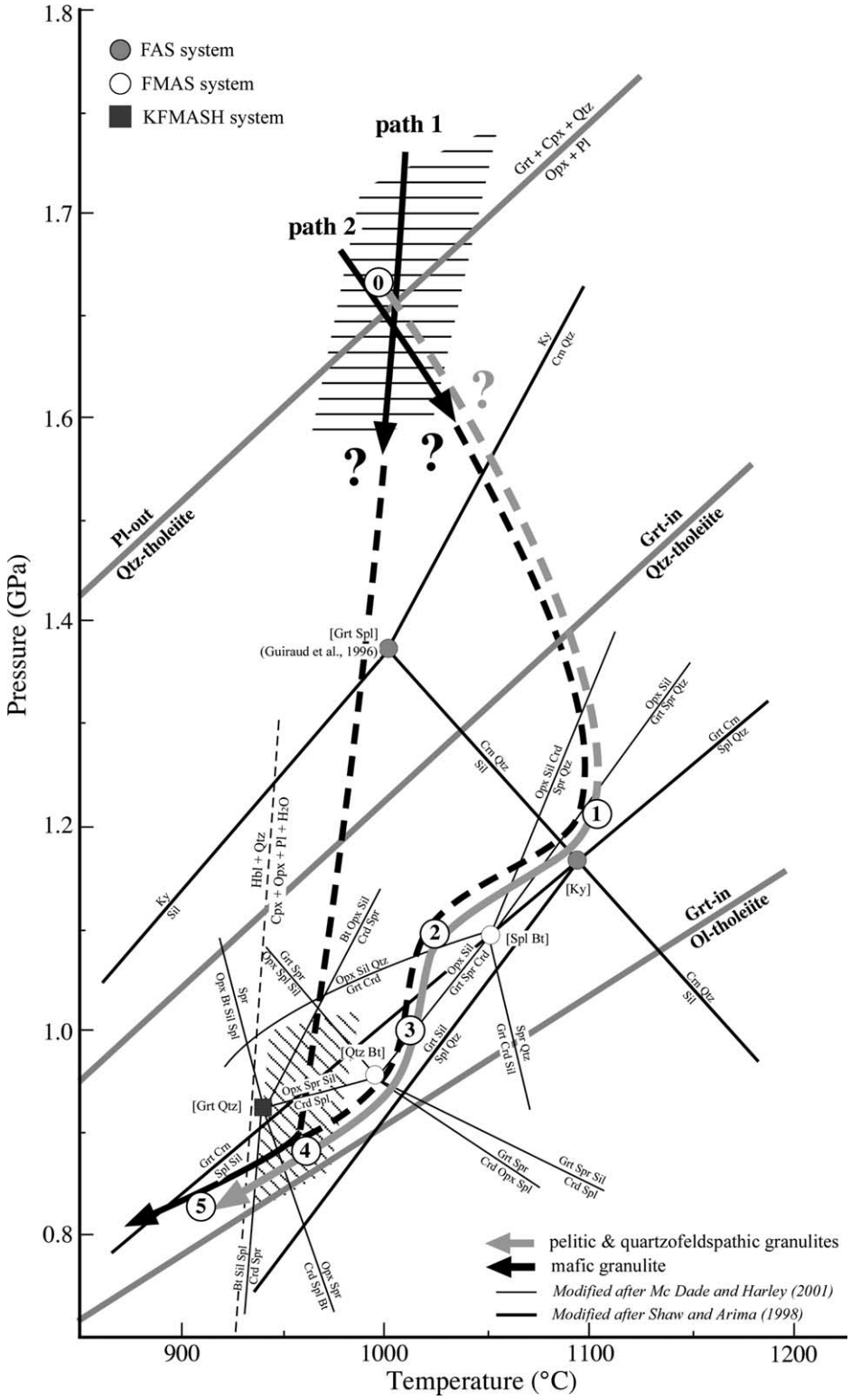

Fig. 9. Reliable P–T path for ultrahigh-temperature metamorphic rocks from the Highland Complex. Stages 1–5 indicate change in divariant assemblages in mafic, pelitic and quartzofeldspathic metamorphic rocks as described in Table 4. Plagioclase-out and garnet-in lines are after Green and Ringwood (1967). Fine dotted line shows hornblende producing univariant line after Spear (1993).

granulite-facies (Motoyoshi and Ishikawa, 1997; Yoshimura et al, 2003). Metamorphic evolution of the ultrahigh-temperature granulites from Rundvågshetta is also assumed to be of nearly isothermal decompression started from kyanite-stabilized high-pressure granulite-facies down to lower-pressure condition through sapphirine + quartz, orthopyroxene + sillimanite + quartz and garnet + cordierite stability fields (Motoyoshi and Ishikawa, 1997; Yoshimura et al., 2003). It has been

considered that the Highland Complex in Sri Lanka was juxtaposed with the Lützow–Holm Complex in east Antarctica during the Gondwana era (e.g. Shiraishi et al., 1994), when widely reported ordinary granulite-facies metamorphism was taken place in both complexes as part of the Pan-African metamorphic event (e.g. Hensen and Zhou, 1997). Therefore, there is remaining a possibility that the specific ultrahigh-temperature/high-pressure granulite-facies metamorphism in the Highland Complex (stages 0 and 1 in Fig. 9) as well as the Lützow–Holm Complex might have taken place before the Pan-African metamorphism during the Gondwana era.

Acknowledgements

We are grateful to M. Brown and S. Bose for their critical and constructive comments. The co-editor, A. Collins is thanked for his comments and editorial support. M. Yoshida, M. Arima and late P.G. Cooray are acknowledged for various assistances during this work. Thanks are also due to H. Kagami, Y. Hiroi, Y. Motoyoshi, Y. Yoshimura, H. Mouri and T. Ando for their collaboration in frequent discussions. This work was partly supported by a Grant-in-Aid for Scientific Research from the Ministry of Education, Science, Sports and Culture, Japan (No. 14340150: Y. Osanai). This is a contribution to IGCP-368 and -440.

References

Ai, Y., 1994. A revision of the garnet-clinopyroxene Fe^{2+}–Mg exchange geothermometer. Contributions to Mineralogy and Petrology 115, 465–473.

Almond, D.C., 1991. Arena Gneiss and Kandy Gneiss—a proposed subdivision of the highland series around Kandy, and its significance. Journal of Geological Society of Sri Lanka 3, 41–50.

Anovitz, L.M., Essene, E.J., Metz, G.W., Bohlen, S.R., Westrum, E.F., Hemingway, B.M., 1993. Heat vapacity and phase equilibria of almandine, $Fe_3Al_2Si_3O_{12}$. Geochimica et Cosmochimica Acta 57, 4191–4204.

Aramaki, S., Roy, R., 1963. A new polymorph of Al_2SiO_5 and further studies in the system Al_2O_3–SiO_2–H_2O. American Mineralogist 48, 1322–1347.

Aranovich, L.Y., Berman, R.G., 1997. A new garnet–orthopyroxene thermometer based on reversed Al_2O_3 solubility in FeO–Al_2O_3–SiO_2 orthopyroxene. American Mineralogist 82, 345–353.

Bhattacharya, A., Krishnakumar, K.R., Raith, M., Sen, S.K., 1991. An improved set of a-X parameters for Fe–Mg–Ca garnets and refinements of the orthopyroxene–garnet thermometer and orthopyroxene–garnet–plagioclase–quartz barometer. Journal of Petrology 32, 629–656.

Bohlen, S.R., Wall, V.J., Boettcher, A.L., 1983. Geobarometry in granulites. In: Saxena, S.K. (Ed.), Kinetics and Equilibrium in Mineral Reactions. Springer, New York, pp. 141–171.

Cooray, P.G., 1984. An Introduction to the Geology of Sri Lanka (Ceylon). National Museum of Sri Lanka, Colombo.

Cooray, P.G., 1994. The Precambrian of Sri Lanka: a historical review. Precambrian Research 66, 3–18.

Droop, G.T.R., 1989. Reaction history of garnet–sapphirine granulites and conditions of archaean high-pressure granulite facies metamorphism in Central Limpopo Belt, Zimbabwe. Journal of Metamorphic Geology 7, 383–403.

Ellis, D.J., Green, E.H., 1979. An experimental study of the effect of Ca upon garnet–clinopyroxene Fe–Mg exchange equilibria. Contributions to Mineralogy and Petrology 71, 13–22.

Goscombe, B., 1992. Silica-undersaturated sapphirine, spinel and kornerupine granulite facies rocks, NE Strangway Range, central Australia. Journal of Metamorphic Geology 10, 181–201.

Green, D.H., Ringwood, A.E., 1967. An experimental investigation of the gabbro to eclogite transformation and its petrological applications. Geochimica et Cosmochimica Acta 31, 767–833.

Guiraud, M., Kienast, J.R., Ouzegane, K., 1996. Corundum–quartz-bearing assemblages in the ihouhaouene area (In Ouzzal Algeria). Journal of Metamorphic Geology 14, 755–762.

Hansen, E.C., Janardhan, A.S., Newton, R.C., Prame, W.B.K.N., Kumar, R., 1987. Arrested charnockite formation in southern India and Sri Lanka. Contributions to Mineralogy and Petrology 96, 225–244.

Harley, S.L., 1984. An experimental study of the partitioning of Fe and Mg between garnet and orthopyroxene. Contributions to Mineralogy and Petrology 86, 359–373.

Harley, S.L., 1998. On the occurrence and characterization of ultrahigh-temperature crustal metamorphism. In: Treloar, P.J., O'Brien, P.J., (Eds.) What Drives Metamorphism and Metamorphic Reactions? Geological Society of London, Special Publication 138, 81–107.

Harley, S.L., Green, D.H., 1982. Garnet–orthopyroxene barometry for granulites and peridotites. Nature 300, 697–701.

Harley, S.L., Motoyoshi, Y., 2000. Alumina-zoning in orthopyroxene in a sapphirine quartzite: evidence for $>1120\,^{\circ}C$ ultrahigh temperature metamorphism in the Napier complex, Enderby Land, Antarctica. Contributions to Mineralogy and Petrology 138, 293–307.

Harlov, D.E., Milke, R., 2002. Stability of corundum + quartz relative to kyanite and sillimanite at high temperature and pressure. American Mineralogist 87, 424–432.

Hensen, B.J., Harley, S.L., 1990. Graphical analysis of P–T–X relations in granulite facies metapelites. In: Ashworth, J.R., Brown, M. (Eds.), High-Temperature Metamorphism and Crustal Anatexis. The Unwin & Hyman, London, pp. 19–56.

Hensen, B.J., Zhou, B., 1997. East Gondwana amalgamation by Pan-African collision? Evidence from Prydz Bay, east Antarctica. In: Ricci, C.A. (Ed.), The Antarctic Region: Geological Evolution and Processes. Terra Antarctica Publication, Siena, pp. 115–119.

Hiroi, Y., Asami, M., Cooray, P.G., Fernando, M.R.D., Jayatileke, J.M.S., Kagami, H., Mathavan, V., Matsueda, H., Motoyoshi, Y., Ogo, Y., Osanai, Y., Owada, M., Perera, L.R.K., Prame, K.B.N., Ranasinghe, N.S., Shiraishi, K., Vitanage, P.W., Yoshida, M., 1990. Arrested charnockite formation in Sri Lanka: field and petrographical evidence for low-pressure conditions. Proceedings of NIPR Symposium on Antarctic Geosciences 4, 213–230.

Hiroi, Y., Ogo, Y., Namba, L., 1994. Evidence for prograde metamorphic evolution of Sri Lankan pelitic granulites, and implications for the development of continental crust. Precambrian Research 66, 245–263.

Kehelpannala, K.V.W., 1991. Structural evolution of high-grade terrain in Sri Lanka with special reference to the Arenas around Dodangaslanda and Kandy. In: Kröner, A. (Ed.), The Crystalline Crust of Sri Lanka, Part I. Geological Survey Department of Sri Lanka, Professional Paper 5, pp. 69–88.

Kehelpannala, K.V.W., 1997. Deformation of a high-grade gondwana fragment, Sri Lanka. Gondwana Research 1, 47–68.

Kehelpannala, K.V.W., 1999. Shear zone-controlled charnockitization, retrogression and metasomatism of high-grade rocks. Gondwana Research 2, 573–577.

Kehelpannala, K.V.W., 2003. Structural evolution of the middle to lower crust in Sri Lanka—a review. Journal of the Geological Society of Sri Lanka 11, 45–86.

Kehelpannala, K.V.W., 2004. Arc accretion around Sri Lanka during the assembly of Gondwana. Gondwana Research 7, 1323–1328.

Kleinschrodt, R., 1994. Large-scale thrusting in the lower crustal basement of Sri Lanka. Precambrian Research 66, 39–57.

Kretz, R., 1983. Symbols for rock-forming minerals. American Mineralogist 68, 277–279.

Kriegsman, L., 1991. Structural geology of the Sri Lankan basement—a preliminary review. In: Kröner, A. (Ed.), The Crystalline Crust of Sri Lanka, Part I. Geological Survey Department of Sri Lanka, Professional Paper 5, pp. 52–68.

Kriegsman, L.M., Schumacher, J.C., 1999. Petrology of sapphirine-bearing and associated granulites from central Sri Lanka. Journal of Petrology 40, 1211–1239.

Krogh, E.J., 1977. Origin and metamorphism of iron formation and associated rocks, Lofoten-Vesterålen, N. Norway, I, the Vestpolltind Fe–Mn deposit. Lithos 10, 243–255.

Krogh, E.J., 1988. The garnet–clinopyroxene Fe–Mg geothermometer—a reinterpretation of existing experimental data. Contributions to Mineralogy and Petrology 99, 44–48.

Krogh, E.J., 2000. The garnet–clinopyroxene Fe^{2+}–Mg thermometer: an updated calibration. Journal of Metamorphic Geology 18, 211–219.

Kröner, A., Cooray, P.G., Vintage, P.W., 1991. Lithotectonic subdivision of the Precambrian basement in Sri Lanka. In: Kröner, A. (Ed.), The Crystalline Crust of Sri Lanka, Part I. Geological Survey Department of Sri Lanka, Professional Paper 5, pp. 5–21.

Kröner, A., Kehelpannala, K.V.W., Hegner, E., 2003. Ca. 700–1000 Ma magmatic events and grenvillian-age deformation in Sri Lanka: relevance for rodinia supercontinent formation and dispersal, and Gondwana amalgamation. Journal of Asian Earth Sciences 22, 279–300.

Lal, R.K., 1993. Internally consistent recalibrations of mineral equilibria for geothermobarometry involving garnet–orthopyroxene–plagioclase–quartz assemblages and their application to the South Indian granulites. Journal of Metamorphic Geology 11, 855–866.

Lee, H.Y., Ganguly, J., 1988. Equilibrium compositions of coexisting garnet and orthopyroxene: experimental determination in the system $FeO–MgO–Al_2O_3–SiO_2$ and applications. Journal of Petrology 29, 93–113.

Liew, T.C., Milisenda, C.C., Hölzl, S., Köhler, H., Hofmann, A.W., 1991. Isotopic characterisation of the high-grade basement rocks of Sri Lanka. In: Kröner, A. (Ed.), The Crystalline Crust of Sri Lanka, Part I. Geological Survey Department of Sri Lanka, Professional Paper 5, pp. 258–267.

McDade, P., Harley, S.L., 2001. A petrogenetic grid for aluminous granulite facies metapelites in the KFMASH system. Journal of Metamorphic Geology 19, 45–59.

Milisenda, C.C., Liew, T.C., Hofmann, A.W., Kröner, A., 1988. Isotopic mapping of age provinces in Precambrian high-grade terrains: Sri Lanka. Journal of Geology 96, 608–615.

Motoyoshi, Y., Ishikawa, M., 1997. Metamorphic and structural evolution of granulites from Rundvågshetta, Lützow–Holm Bay, east Antarctica. In: Ricci, C.A. (Ed.), The Antarctic Region: Geological Evolution and Processes. Terra Antarctica Publication, Siena, pp. 65–72.

Mouri, H., Guiraud, M., Osanai, Y., 2004. Review on 'corundum + quartz' assemblage in nature: possible indicator of ultra-high temperature conditions? Journal of Mineralogical and Petrological Sciences 99, 159–163.

Newton, R.C., Perkins III., D., 1982. Thermodynamic calibration of geobarometers based on the assemblages garnet–plagioclase–orthopyroxene (clinopyroxene)–quartz. American Mineralogist 67, 203–222.

Ogo, Y., Hiroi, Y., Prame, K.B.N., Motoyoshi, Y., 1992. A new insight of possible correlation between the Lützow–Holm bay granulites (East Antarctica) and Sri Lankan granulites. In: Yoshida, Y., Kaminuma, K., Shiraishi, K. (Eds.), Recent Progress in Antarctic Earth Science. TERRAPUB, Tokyo, pp. 75–86.

Osanai, Y., 1989. A preliminary report on sapphirine/kornerupine granulite from Highland series, Sri Lanka (extended abstract). Seminar on Recent Advantages in Precambrian Geology of Sri Lanka, IFS Kandy.

Osanai, Y., Ando, K.T., Miyashita, Y., Kusachi, I., Yamasaki, T., Doyama, D., Prame, W.K.B.N., Jayatilake, S., Mathavan, V., 2000. Geological field work in the southwestern and central parts of the Highland complex, Sri Lanka during 1998–1999, special reference to the highest grade metamorphic rocks. Journal of Geoscience, Osaka City University 43, 227–247.

Powell, R., 1985. Regression diagnostic robust regression in geothermometer/geobarometer calibration: the garnet–clinopyroxene geothermometer revisited. Journal of Metamorphic Geology 3, 33–42.

Raase, P., Schenk, V., 1994. Petrology of granulite facies metapelites of the Highland complex, Sri Lanka: implication for the metamorphic zonation and the P–T path. Precambrian Research 66, 265–294.

Raith, M., Faulhaber, S., Hoffbauer, R., Spiering, B., 1991. Characterization of high-grade metamorphism in the southern part of Sri Lanka. In: Kröner, A. (Ed.), The Crystalline Crust of Sri Lanka, Part I, Summary of Research of the German–Sri Lankan Consortium. Geological Survey Department, Sri Lanka, Professional Paper 5, pp. 164–177.

Sajeev, K., Osanai, Y., 2004a. Ultrahigh-temperature metamorphism (1150 °C, 12 kbar) and multi-stage evolution of Mg-, Al-rich granulites from the central Highland Complex, Sri Lanka. Journal of Petrology 45, 1821–1844.

Sajeev, K., Osanai, Y., 2004b. Osumilite and spinel + quartz from Sri Lanka: implications for UHT conditions and retrograde P–T path. Journal of Mineralogical and Petrological Sciences 99, 320–327.

Schenk, V., Raase, P., Schumacher, R., 1988. Very high temperature and isobaric cooling before tectonic uplift in the Highland series of Sri Lanka. Terra Cognita 8, 265.

Schenk, V., Raase, P., Schumacher, R., 1991. Metamorphic zonation and P–T history of the Highland Complex in Sri Lanka. In: Kröner, A. (Ed.), The Crystalline Crust of Sri Lanka, Part I. Geological Survey Department of Sri Lanka, Professional Paper 5, 150–163.

Schumacher, R., Faulhaber, S., 1994. Summary and discussion of P–T estimates from garnet–pyroxene–plagioclase–quartz-bearing granulite-facies rocks from Sri Lanka. Precambrian Research 66, 295–308.

Schumacher, R., Schenk, V., Raase, P., Vitanage, P.W., 1990. Granulite facies metamorphism of matabasic and intermediate rocks in the highland series of Sri Lanka. In: Ashworth, J.R., Brown, M., (Eds.) High-temperature Metamorphism and Crustal Anatexis. The Mineralogical Society Series 2, 235–271.

Seifert, F., 1975. Boron-free kornerupine; a high-pressure phase. American Journal of Science 275, 57–87.

Sen, S.K., Bhattacharya, A., 1984. An orthopyroxene-garnet thermometer and its application to the Madras charnockites. Contributions to Mineralogy and Petrology 88, 64–71.

Shaw, R.K., Arima, M., 1998. A corundum–quartz assemblage from the eastern ghats granulite belt: evidence for high P–T metamorphism? Journal of Metamorphic Geology 16, 189–196.

Shiraishi, K., Ellis, D.J., Hiroi, Y., Fanning, C.M., Motoyoshi, Y., Nakai, Y., 1994. Cambrian orogenic belt in east Antarctica and Sri Lanka: implications for gondwana assembly. Journal of Geology 102, 47–65.

Spear, F.S., 1993. Metamorphic phase equilibria and pressure–temperature–time paths. Mineralogical Society of America, Monograph, 393–446.

Vitanage, P.W., 1972. Post-Precambrian uplifts and regional neotectonic movements in Ceylon. 24th Internatinal Geological Congress, Montreal, Canada, Section 3, pp. 642–654.

Willbold, M., Hegner, E., Kleinschrodt, R., Stosch, H.-G., Kehelpannala, K.V.W., Dulski, P., 2004. Geochemical evidence for a neoproterozoic magmatic continental margin in Sri Lanka—relevance for the Rodinia–Gondwana supercontinent cycle. Precambrian Research 130, 185–198.

Wood, B.J., 1974. The solubility of orthopyroxene co-existing with garnet. Contributions to Mineralogy and Petrology 46, 1–15.

Yoshida, M., Tani, Y., Rajesh, H.M., Santosh, M., Arima, M., 2003. A commentary on Grenvillian events in Sri Lanka. In: Kehelpannala, K.V.W. (Ed.), Proceedings of the IGCP-440 and LEGENDS International Symposium and Field Workshop on 'The Role of Sri Lanka in Rodinia and Gondwana Assembly and Break-Up' March–April. Centenary Publication, Geological Survey & Mines Bureau, Sri Lanka, pp. 9–10.

Yoshimura, Y., Motoyoshi, Y., Miyamoto, T., 2003. Sapphirine-bearing garnet–orthopyroxene granulite from Rundvågshetta in the Lützow-Holm Complex, East Antarctica. Abstract of the 23rd Symposium on Antarctic Geosciences, National Institute of Polar Research, Japan, p.74.